nature cell biology

SCF^{Fbxo9} and CK2 direct the cellular response to growth factor withdrawal via Tel2/Tti1 degradation and promote survival in multiple myeloma

Vanesa Fernández-Sáiz[1,7], Bianca-Sabrina Targosz[1,7], Simone Lemeer[2], Ruth Eichner[1], Christian Langer[3], Lars Bullinger[3], Clemens Reiter[1], Julia Slotta-Huspenina[4], Sonja Schroeder[1], Anna-Maria Knorn[1], Julia Kurutz[1], Christian Peschel[1], Michele Pagano[5], Bernhard Kuster[2,6] and Florian Bassermann[1,8]

The Tel2 (also known as Telo2) and Tti1 proteins control the cellular abundance of mammalian PIKKs and are integral components of mTORC1 and mTORC2. Here we report that Tel2 and Tti1 are targeted for degradation within mTORC1 by the SCF^{Fbxo9} ubiquitin ligase to adjust mTOR signalling to growth factor availability. This process is primed by CK2, which translocates to the cytoplasm to mediate mTORC1-specific phosphorylation of Tel2/Tti1, subsequent to growth factor deprivation. As a consequence, mTORC1 is inactivated to restrain cell growth and protein translation whereas relief of feedback inhibition activates the PI(3)K/TORC2/Akt pathway to sustain survival. Significantly, primary human multiple myelomas exhibit high levels of Fbxo9. In this setting, PI(3)K/TORC2/Akt signalling and survival of multiple myeloma cells is dependent on Fbxo9 expression. Thus, mTORC1-specific degradation of the Tel2 and Tti1 proteins represents a central mTOR regulatory mechanism with implications in multiple myeloma, both in promoting survival and in providing targets for the specific treatment of multiple myeloma with high levels of Fbxo9 expression.

Protein synthesis, cell growth and survival are highly regulated and coordinated events[1]. When deprived of nutrients and mitogens, cells restrain processes that consume resources to favour pathways that promote survival. How cells orchestrate this response is still poorly understood. The PI(3)K-related kinase (PIKK) family member mTOR functions within two distinct multisubunit complexes, mTORC1 and mTORC2. mTORC1 controls cell growth and protein synthesis by phosphorylating S6 kinase 1 (S6K1) and eIF-4E-binding protein 1 (4E-BP-1), whereas mTORC2 regulates cell survival by phosphorylating downstream effectors such as Akt and SGK1 (refs 2,3). mTORC1 signalling through S6K1 negatively regulates Akt by inhibiting the activation of PI(3)K, an upstream activator of Akt. This negative feedback loop probably accounts for the observed activation of Akt on treatment of cells with the mTORC1 inhibitor rapamycin and may be responsible for the limited success of mTORC1 inhibitory drugs in cancer treatment[4,5].

Recently, Tel2 (telomere maintenance 2) and Tti1 (Tel2 interacting protein 1) proteins have been identified to interact with all known mammalian PIKKs and essentially regulate their abundance. The PIKK family comprises mTOR as well as ATM, ATR, DNA-PKcs, SMG-1 and TRRAP. Both post-translational modifications and transcriptional regulation have been largely excluded as regulatory means by which Tel2/Tti1 proteins control PIKK abundance[6,7]. Instead it was suggested that Tel2/Tti1 mediate assembly and maturation of PIKKs (refs 6–9). With regard to mTOR, Tel2 and Tti1 proteins are not only crucial for protein stability, but constitute essential components of both mTORC1 and mTORC2 complexes that are vital for their assembly[7–10].

The ubiquitin proteasome system (UPS) mediates proteolysis of key eukaryotic cell regulatory proteins[11]. E3 ubiquitin-protein ligases are critical in this system, as they allow the transfer of activated ubiquitin from E2 enzymes to the target protein and mediate the specificity of substrate recognition[11,12]. The Skp1–Cul1–F-box protein (SCF) complexes are the prototypical multisubunit E3 ubiquitin ligases, which are composed of invariable core components (Cul1, Skp1 and Roc1) and a variable F-box protein, which specifically recruits substrates[13–15].

[1]Department of Medicine III, Klinikum rechts der Isar, Technische Universität München, Ismaninger Strasse 22, 81675 Munich, Germany. [2]Department of Proteomics and Bioanalytics, Technische Universität München, Emil Erlenmeyer Forum 5, 85354 Freising, Germany. [3]Department of Internal Medicine III, University of Ulm, Albert Einstein Allee 23, 89081 Ulm, Germany. [4]Department of Pathology, Klinikum rechts der Isar, Technische Universität München, Troger Strasse 18, 81675 Munich, Germany. [5]Department of Pathology, NYU Cancer Institute, New York University School of Medicine, 522 First Avenue, SRB 1107 New York, New York 10016, USA. [6]Center for Integrated Protein Science Munich (CIPSM), Emil Erlenmeyer Forum 5, 85354 Freising, Germany. [7]These authors contributed equally to this work. [8]Correspondence should be addressed to F.B. (e-mail: florian.bassermann@lrz.tum.de)

Received 3 September 2012; accepted 9 November 2012; published online 23 December 2012; DOI: 10.1038/ncb2651

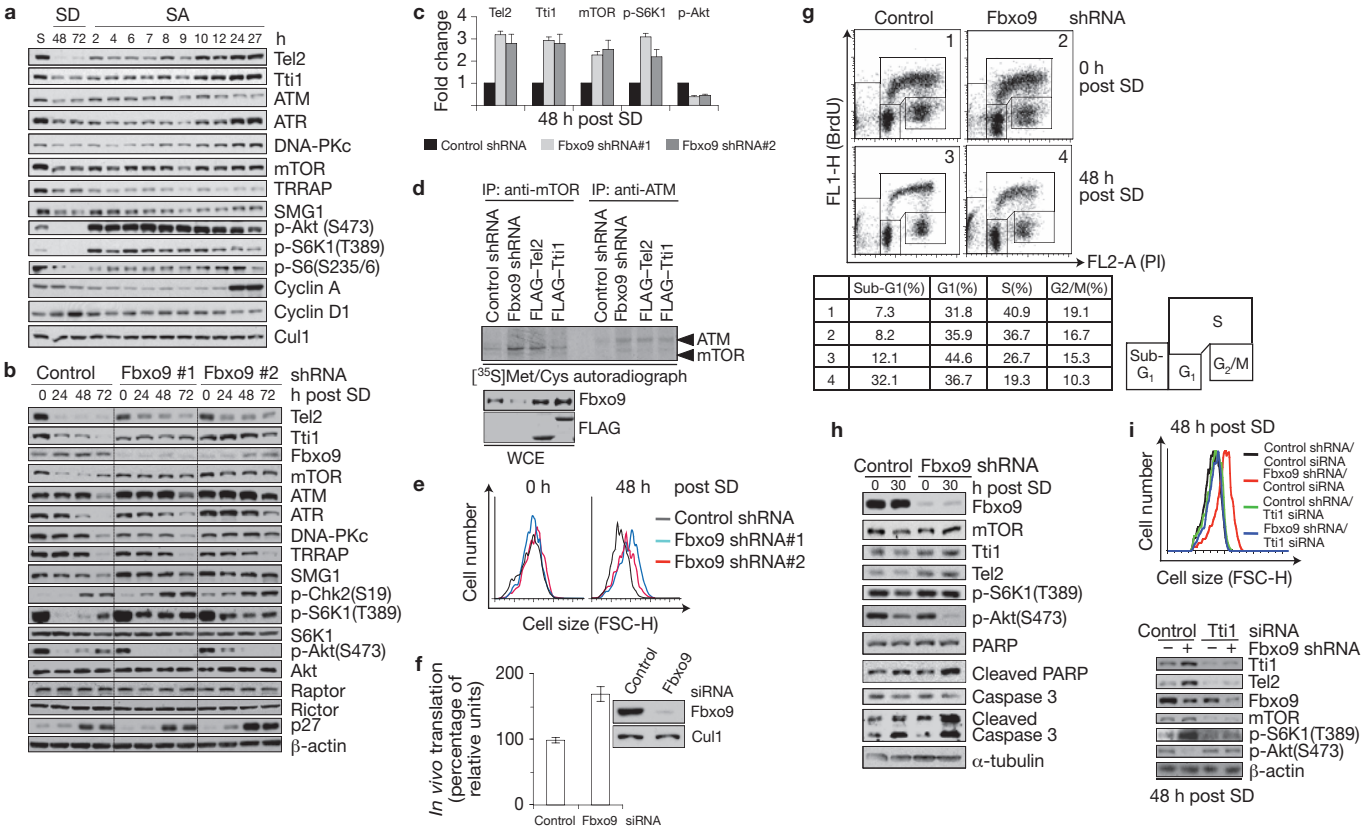

Figure 1 Fbxo9 mediates degradation of the Tel2 and Tti1 proteins in response to serum withdrawal to regulate mTOR abundance and function. (**a**) T98G cells were either grown in the presence of serum (S: 10% FBS) or deprived of serum (SD: 0.02% FBS) for up to 72 h. After this period, serum was added (SA: 10% FBS). Protein extracts were analysed by immunoblotting with antibodies against the indicated proteins. (**b**) T98G cells were infected with shRNA constructs directed against a non-relevant mRNA or against two distinct sequences of Fbxo9 mRNA. Cells were grown in normal medium (S) or deprived of serum (SD) for the indicated times. Protein extracts were then prepared and probed with antibodies as specified. (**c**) Quantification of proteins shown in **b** at the 48 h time point averaged with two additional, independent experiments. The value given for the amount of protein present in the control sample (S) was set as 1. Error bars represent s.d., $n = 3$. (**d**) Upper panel, U2OS cells retrovirally infected with either shRNA or expression constructs as indicated were serum starved, pulse labelled with [^{35}S]Met/Cys for 2 h and subsequently subjected to immunoprecipitations (IP). Lower panel, immunoblots of whole-cell extracts (WCE). (**e**) Forward scatter analyses of G1-phase gated cells used in **b** were performed to determine cell size. (**f**) HEK293T cells were transfected with a pCMV-SL-LUC reporter plasmid together with a pRL-null *Renilla* plasmid and siRNA oligonucleotides as indicated. Cells were serum starved (SD: 0.1% FBS) for 48 h, and luciferase activities were measured. Error bars represent s.d., $n = 3$. Fbxo9 protein levels are shown in the right panel. (**g**) Cells described in **b** were processed for two-dimensional cell-cycle analysis (BrdU/PI) at the indicated time points. (**h**) HeLa cells expressing either control or Fbxo9 shRNA were deprived of serum for 30 h (SD: 0% FBS) to induce apoptosis. Whole-cell extracts were then analysed with antibodies against the indicated proteins. (**i**) T98G cells expressing either control or Fbxo9 shRNA were transfected with siRNA oligonucleotides as indicated and deprived of serum for 48 h (SD: 0.02% FBS). Top, cell size was assessed using forward scatter analyses as in **e**. Bottom, whole-cell extracts were processed for immunoblotting using the specified antibodies. Uncropped images of blots/gels are shown in Supplementary Fig. S9.

Approximately 70 F-box proteins exist in mammals, yet most remain to be matched to specific substrates[15].

The UPS has also been appreciated as a promising therapeutic target in cancer, particularly in multiple myeloma (MM), the second most common haematologic malignancy[16]. Indeed, the proteasome inhibitor bortezomib has been well established in the first-line treatment of this disease[17], and survival pathways in MM have been shown to be positively regulated by ubiquitin-mediated degradation[18,19]. The identity of individual deregulated ubiquitylation reactions in MM has however remained largely unknown.

Here, we have identified a mechanism by which the evolutionarily highly conserved, yet orphan SCF^{Fbxo9} ubiquitin ligase directs the cellular response to growth factor withdrawal to switch to a state of nutritional saving and maintenance of survival. By targeting Tel2 and Tti1 proteins specifically within mTORC1 in a CK2-dependent manner, Fbxo9 attenuates mTORC1 signalling while sustaining mTORC2 signalling through relief of feedback inhibition. When Fbxo9 is overexpressed, as we show is the case in 30% of the samples within a cohort of 180 myeloma patients, this mechanism is driven towards constitutive activation of the PI(3)K/mTORC2/Akt pathway to promote survival.

RESULTS

Fbxo9 mediates degradation of Tel2 and Tti1 proteins in response to serum withdrawal to regulate mTOR abundance and function

To identify biologically relevant substrates of Fbxo9, we conducted an unbiased screen that combined tandem affinity purification (TAP) with mass spectrometric analyses. In addition to peptides derived from the SCF core components Cul1 and Skp1, ten unique peptides

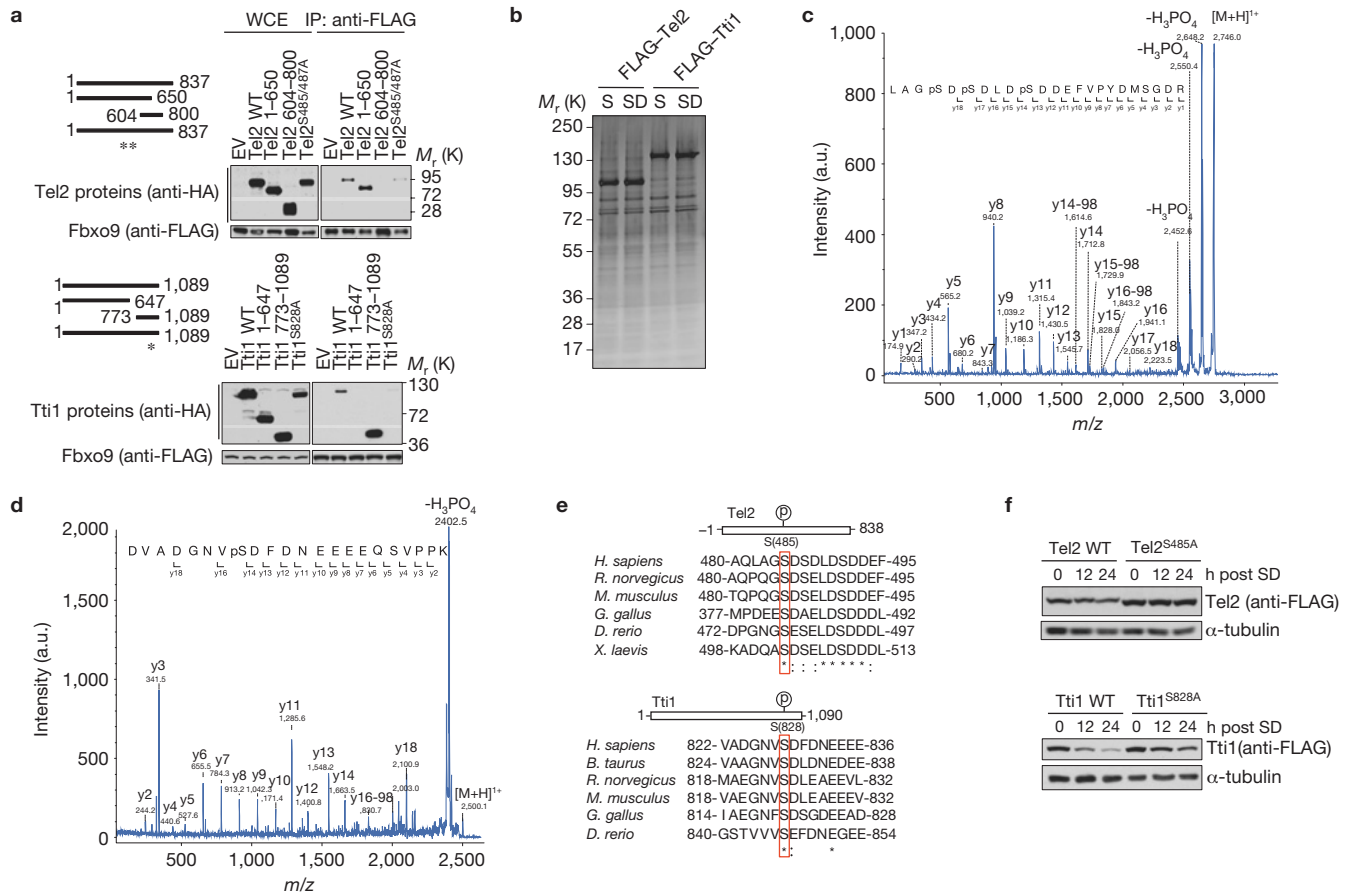

Figure 2 Identification of the Fbxo9-specific phospho-degrons in Tel2 and Tti1. (**a**) HEK293T cells were co-transfected with FLAG-tagged Fbxo9 and the indicated HA-tagged deletion or point mutants of Tel2 and Tti1. Whole-cell extracts (WCE) were immunoprecipitated (IP) with an anti-FLAG antibody, and the indicated proteins were detected by immunoblotting. EV, empty vector. (**b**) FLAG-tagged Tel2 and Tti1 were expressed in HEK293T cells. At 24 h post transfection, cells were either cultured in normal serum (S: 10% FBS) or deprived of serum for 5 h (SD: 0.02% FBS). Thereafter, whole-cell extracts were prepared and processed for immunoprecipitation with anti-FLAG beads and subsequent elution with 3x-FLAG–octapeptide. The eluate was then processed for mass spectrometric analysis of protein phosphorylation. The depicted gel corresponds to 5% of the final FLAG–eluates visualized by silver staining. (**c**) The peptide LAGSDSDLDSDDEFVPYDMSGDR of Tel2 is triply phosphorylated, as indicated by three major neutral losses of H_3PO_4 after fragmentation of the precursor peptide mass. Phosphorylation can readily be assigned to residues Ser 485, Ser 487 and Ser 491 as the indicative fragment ions y13, y14 and y18 are clearly present in the tandem mass spectrometry spectrum. (**d**) The peptide DVADGNVSDFDNEEEEQSVPPK of Tti1 is phosphorylated, as indicated by the major neutral losses of H_3PO_4 after fragmentation of the precursor peptide mass. Phosphorylation can readily be assigned to residue S828 as the indicative fragment ions y14 and y16 are clearly present in the tandem mass spectrometry spectrum. (**e**) CLUSTAL W alignments of the candidate phospho-degrons in Tel2 and Tti1. Identical residues (*); conservative residue differences (:). (**f**) HEK293T cells were transfected with constructs expressing wild-type (WT) or mutant forms of Tel2 and Tti1, which are deficient in Fbxo9 binding. Cells were subsequently deprived of serum (SD: 0.1% FBS) for the indicated times, and processed for immunoblotting with the specified antibodies. Uncropped images of blots/gels are shown in Supplementary Fig. S9.

corresponding to Tel2 and five unique peptides corresponding to Tti1 were identified (Supplementary Fig. S1).

As Tel2 and Tti1 regulate the abundance of PIKKs, we analysed Tel2/Tti1 expression in response to a series of PIKK-activating/inactivating stimuli. These experiments identified a decrease in Tel2/Tti1 expression levels in response to growth factor withdrawal, whereas after growth factor stimulation, levels increased (Fig. 1a). Messenger RNA levels of Tel2/Tti1 remained unchanged, whereas treatment with MG132 prevented the disappearance of Tel2 and Tti1, suggesting protein degradation by the UPS (Supplementary Fig. S2). Notably, the destabilization of Tel2/Tti1 paralleled decreased expression of different PIKKs, particularly mTOR (Fig. 1a).

The interaction between Tel2/Tti1 and Fbxo9 identified by mass spectrometry suggests that SCF^{Fbxo9} is probably the ubiquitin ligase that mediates degradation of both proteins. Consistent with this possibility, Fbxo9 was the only F-box protein (among five tested) that co-immunoprecipitated with endogenous Tel2/Tti1 proteins (Supplementary Fig. S3a). Reciprocal experiments confirmed that endogenous Fbxo9 specifically co-immunoprecipitated with both Tel2 and Tti1 (Supplementary Fig. S3b). Binding of Tel2/Tti1 to Fbxo9 was impaired under conditions of mitogenic stimulation (Supplementary Fig. S3c), consistent with an increase in Tel2/Tti1 expression under this condition (Fig. 1a). In addition, indirect immunofluorescence microscopy studies revealed co-localization of Tel2 and Tti1 with Fbxo9 particularly under conditions of serum withdrawal (Supplementary Fig. S3d).

To further investigate whether Fbxo9 may regulate the stability of Tel2 and Tti1, we used two different small hairpin RNA (shRNA) constructs to silence the expression of Fbxo9. Depletion of Fbxo9 using either shRNA inhibited the degradation of Tel2 and Tti1 after

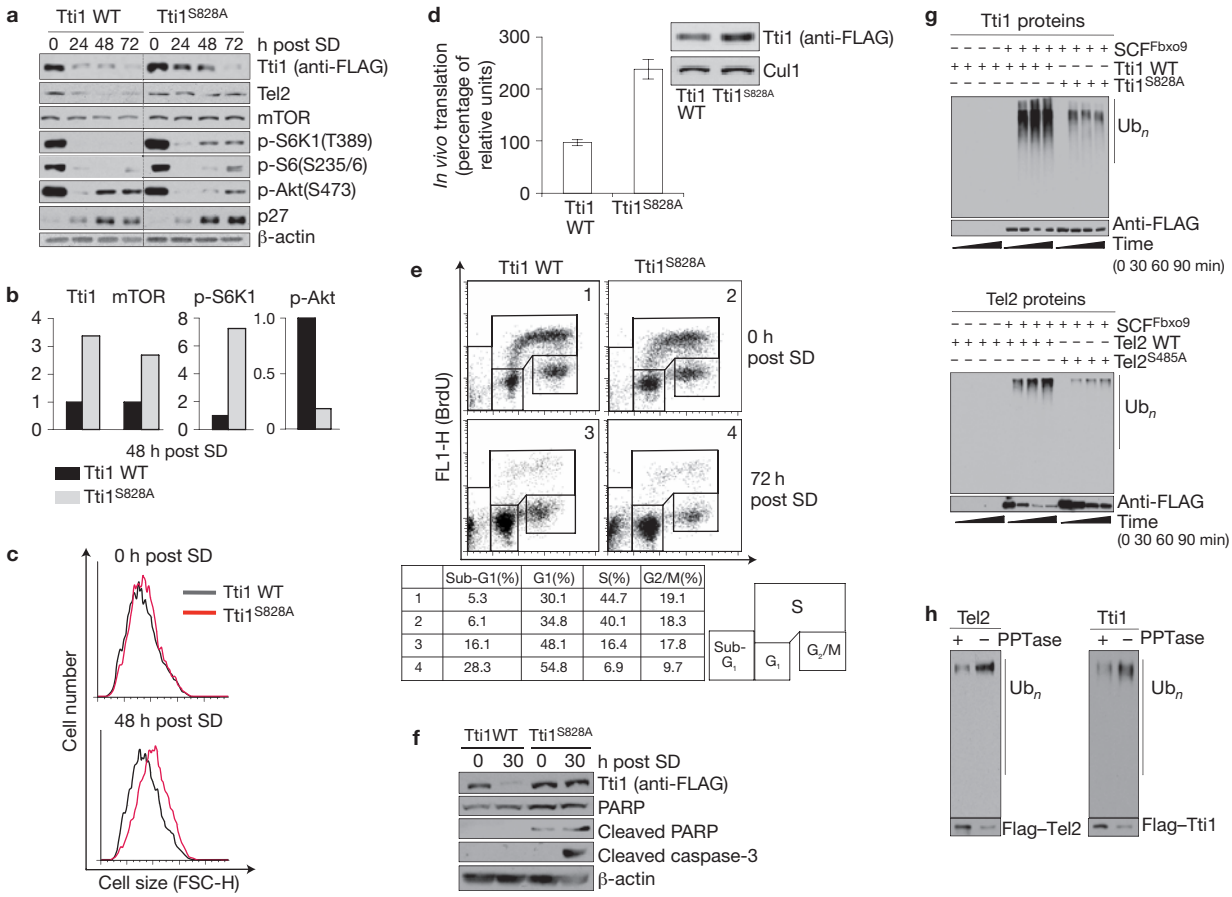

Figure 3 Phospho-degron-dependent ubiquitylation of Tel2 and Tti1 via Fbxo9 regulates mTOR signalling (**a**) T98G cells were retrovirally infected with the indicated constructs, treated as described in Fig. 1b and collected at the indicated time points. Immunoblotting was performed with antibodies against the specified proteins. WT, wild type. (**b**) The graphs show the quantification of Tti1, mTOR, phospho-S6K1 and phospho-Akt levels shown in **a** at the 48 h time point averaged with an additional, independent experiment ($n = 2$). (**c**) Forward scatter analyses were performed on G1-phase gated cells used in **a** to determine cell size. (**d**) HEK293T cells were transfected with a pCMV-SL-LUC reporter plasmid together with a pRL-null *Renilla* luciferase plasmid and expression vectors as indicated. Cells were serum starved (SD: 0.1% FBS) for 48 h, and luciferase activities were measured by a dual-luciferase assay. Error bars represent s.d., $n = 3$. Tti1 protein levels are shown in the right panel. (**e**) Cells described in **a** were processed for two-dimensional cell-cycle analysis (BrdU/PI) at the indicated time points. (**f**) HeLa cells were retrovirally infected to express the indicated forms of Tti1, deprived of serum (SD: 0% FBS) to induce apoptosis, and subjected to immunoblot analyses with the indicated antibodies. (**g**) *In vitro* ubiquitylation assays of the Tel2 and Tti1 proteins were conducted in the presence of purified Skp1–Cul1–Roc1 complex and E1/E2 enzymes, and in the presence or absence of Fbxo9. The bracket on the right-hand side marks polyubiquitylated Tel2 or Tti1. (**h**) *In vitro* ubiquitylation assays of Tel2 and Tti1 were performed as in **g** except that purified Fbxo9 was included in all samples and λ-phosphatase (PPTase) was added as indicated. Uncropped images of blots/gels are shown in Supplementary Fig. S9.

serum withdrawal (Fig. 1b,c). Stabilization of Tel2 and Tti1 was associated with increased expression levels of different PIKKs (Fig. 1b,c and Supplementary Fig. S2a,b). This effect was most prominent for mTOR, in line with its most marked loss of abundance in response to serum withdrawal. Stabilization of Tel2/Tti1 and mTOR resulted in sustained phosphorylation of the mTORC1 substrate S6K1, whereas phosphorylation of Akt, an mTORC2 substrate, was further restrained suggesting a direct effect on mTORC1 signalling (Fig. 1b,c and Supplementary Fig. S2a,b). Similar results were obtained in serum-starved primary human IMR90 fibroblasts (Supplementary Fig. S4). In addition, we found an increase in the level of *de novo*-synthesized mTOR (and ATM) protein on knockdown of Fbxo9 (Fig. 1d). This result is in line with previous observations, which demonstrate decreased *de novo* synthesis of ATM and mTOR in *Tel2*$^{-/-}$ mouse embryonic fibroblasts[6]. To further analyse the effect of Fbxo9 loss on mTOR signalling, we examined cell growth, mRNA translation, proliferation and survival as readouts of mTORC1 and mTORC2. Cells treated to downregulate Fbxo9 were larger than control cells (Fig. 1e) and demonstrated increased levels of cap-dependent translation of a luciferase mRNA with a stem–loop-structured 5′-UTR (Fig. 1f), indicative of increased mTORC1 signalling. Conversely, BrdU uptake and cell survival were decreased in serum-starved Fbxo9-knockdown cells, suggesting further loss of mTORC2 signalling (Fig. 1g,h). Deletion of Fbxo9 gave rise to specific phenotypes only in the presence of Tel2/Tti1, indicating that Fbxo9-regulated alterations in mTORC1 and mTORC2 signalling depend on the modulation of Tel2/Tti1 (Fig. 1i).

Phospho-degron-dependent ubiquitylation of Tel2 and Tti1 via Fbxo9 regulates mTOR signalling

In contrast to other ligases, such as APC/C, most SCF substrates are recognized by the F-box protein on post-translational modification, usually through phosphorylation of a specific degron motif[14,20]. To

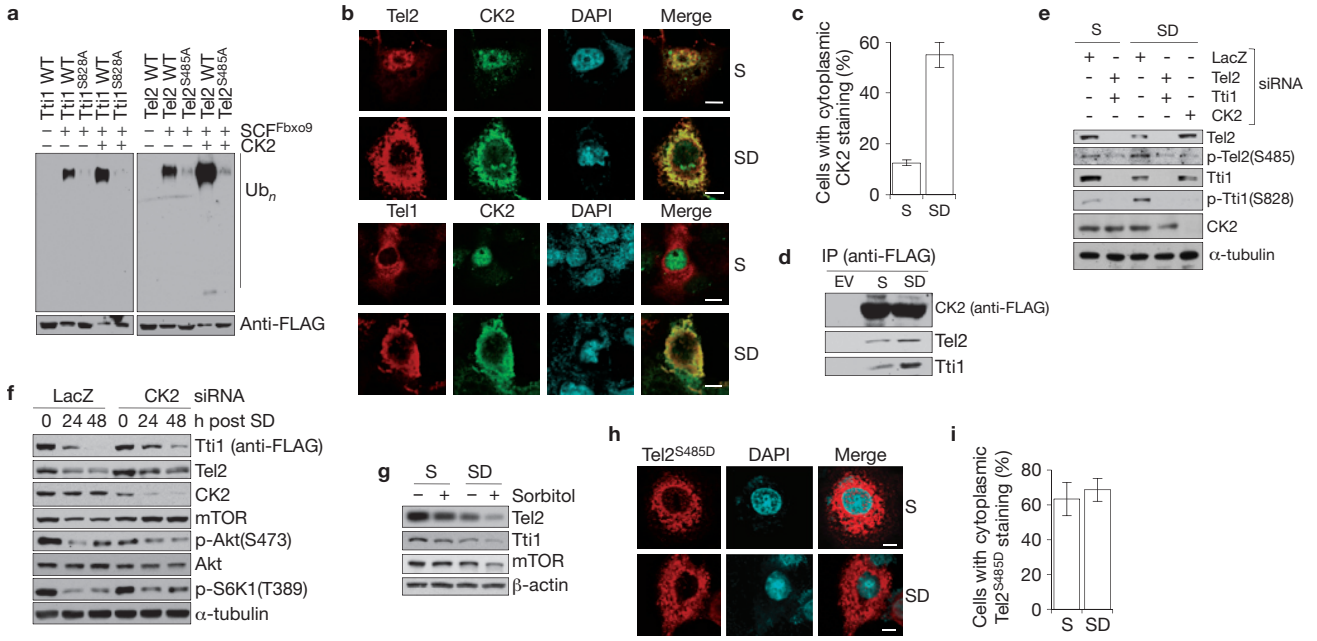

Figure 4 CK2 associates with Tel2 and Tti1 on growth factor withdrawal to mediate their phospho-degron-specific phosphorylation and Fbxo9-dependent degradation. (**a**) *In vitro* ubiquitylation assays were performed as in Fig. 3g except that purified CK2 was added as specified. WT, wild type. (**b**) COS7 cells were transiently transfected with plasmids encoding FLAG–CK2 and either HA–Tti1 or HA–Tel2. Cells were then cultured in normal serum (S: 10% FBS) or deprived of serum for 5 h (SD: 0.02% FBS). Thereafter, cells were fixed with methanol and incubated with anti-FLAG antibody (green) and anti-HA antibody (red). DNA was stained with DAPI (blue). Scale bars, 10 μm. (**c**) Quantification of cells shown in **b** with cytoplasmic CK2 fluorescence staining grown under serum-containing or serum-deprived conditions. Error bars represent s.d., $n = 3$. (**d**) HEK293T cells were transfected with either empty vector (EV) or a FLAG–CK2α expression plasmid. Cells were then serum starved (SD: 0.1% FBS) for 48 h as indicated, and anti-FLAG immunoprecipitations (IP) were performed thereafter. Bound fractions were analysed as indicated. (**e**) T98G cells were transfected with siRNA oligonucleotides as indicated, either grown under serum-containing (S: 10% FBS) or serum-deprived (SD: 0.02% FBS) conditions, and subjected to immunoblot analyses with the indicated antibodies. (**f**) T98G cells were treated with siRNAs directed against CK2, deprived of serum (SD: 0.02% FBS) for the indicated time points and processed for immunoblotting. (**g**) T98G cells were cultured under normal serum (S: 10% FBS) or serum deprived (SD: 0.02% FBS) conditions, treated with sorbitol as indicated and subjected to immunoblot analyses. (**h**) COS7 cells were transiently transfected with a plasmid encoding HA–Tel2^{S485D} and subsequently treated and visualized as in **b**. Scale bars, 10 μm. (**i**) Quantification of the cells shown in **h** with cytoplasmic Tel2^{S485D} fluorescence staining grown under serum-containing or serum-deprived conditions. Error bars represent s.d., $n = 3$. Uncropped images of blots/gels are shown in Supplementary Fig. S9.

identify the Fbxo9-specific degrons of Tel2 and Tti1, we combined a series of binding experiments using Tel2/Tti1 deletion mutants, and phosphorylation analysis by mass spectrometry (Fig. 2a–d). These experiments identified the evolutionarily conserved motifs ^{485}pSDSDL^{489} of Tel2 and ^{828}pSDFDN^{833} of Tti1 as the relevant binding sites (Fig. 2e). Whereas Ser 828 was the only residue found to be phosphorylated in Tti1, we identified Tel2 phosphorylation at Ser 487 and Ser 491, in addition to Ser 485 (Fig. 2c,d). This finding is in line with a previous report, which demonstrated phosphorylation of Ser 487 and Ser 491 (ref. 9). Accordingly, forms of Tel2 and Tti1 mutated at the respective serine residues retained stability in serum-deprived cells, indicating that phosphorylation of the Fbxo9-specific degrons of Tel2 and Tti1 is necessary for their efficient degradation (Figs 2f and 3a,b). Notably, expression of Tti1^{S828A} maintained mTOR expression, increased phosphorylation of S6K1 and S6, and further decreased Akt phosphorylation on serum deprivation, indicative of mTORC1 activation and mTORC2 inactivation (Fig. 3a,b). Likewise, an increase in cell size and cap-dependent translation, yet a decrease in proliferation and survival was observed in cells expressing Tti1^{S828A} (Fig. 3c–f), in line with our knockdown experiments.

Next, we reconstituted ubiquitylation of Tel2 and Tti1 *in vitro*. Wild-type forms of the proteins, but not the Tel2^{S485A} and Tti1^{S828A} mutants, were efficiently ubiquitylated in the presence of Fbxo9 (Fig. 3g and Supplementary Fig. S5a). Likewise, λ-phosphatase treatment inhibited Fbxo9-mediated *in vitro* ubiquitylation of Tel2 and Tti1, further demonstrating the need of phosphorylation for the Fbxo9-mediated degradation process (Fig. 3h). Moreover, *in vivo* ubiquitylation assays demonstrated increased ubiquitylation levels of Tel2 and Tti1 in cells overexpressing Fbxo9 (Supplementary Fig. S5b).

CK2 associates with Tel2 and Tti1 on growth factor withdrawal to mediate degron-specific phosphorylation and Fbxo9-dependent degradation

Sequence alignments revealed that both degron motifs of Tel2 and Tti1 represent canonical phosphorylation sites for CK2(SxxD/E). Indeed, phosphorylation of Tel2 on Ser 485 and Tti1 on Ser 828 by CK2 was confirmed in kinase assays using purified proteins, and *in vitro* binding of Tel2 and Tti1 to Fbxo9 was dependent on CK2-mediated degron phosphorylation (Supplementary Fig. S6a,b). *In vitro* ubiquitylation of wild-type Tel2 and Tti1 was enhanced on addition of purified CK2, whereas the Tel2^{S485A} and Tti1^{S828A} mutants remained unaffected (Fig. 4a). We next investigated how CK2 could mediate phosphorylation of Tel2 and Tti1 specifically in the context of growth factor withdrawal, as CK2 is considered to be constitutively active and its regulation is poorly understood[21]. We did not detect any significant changes in the intrinsic *in vitro* kinase activity of

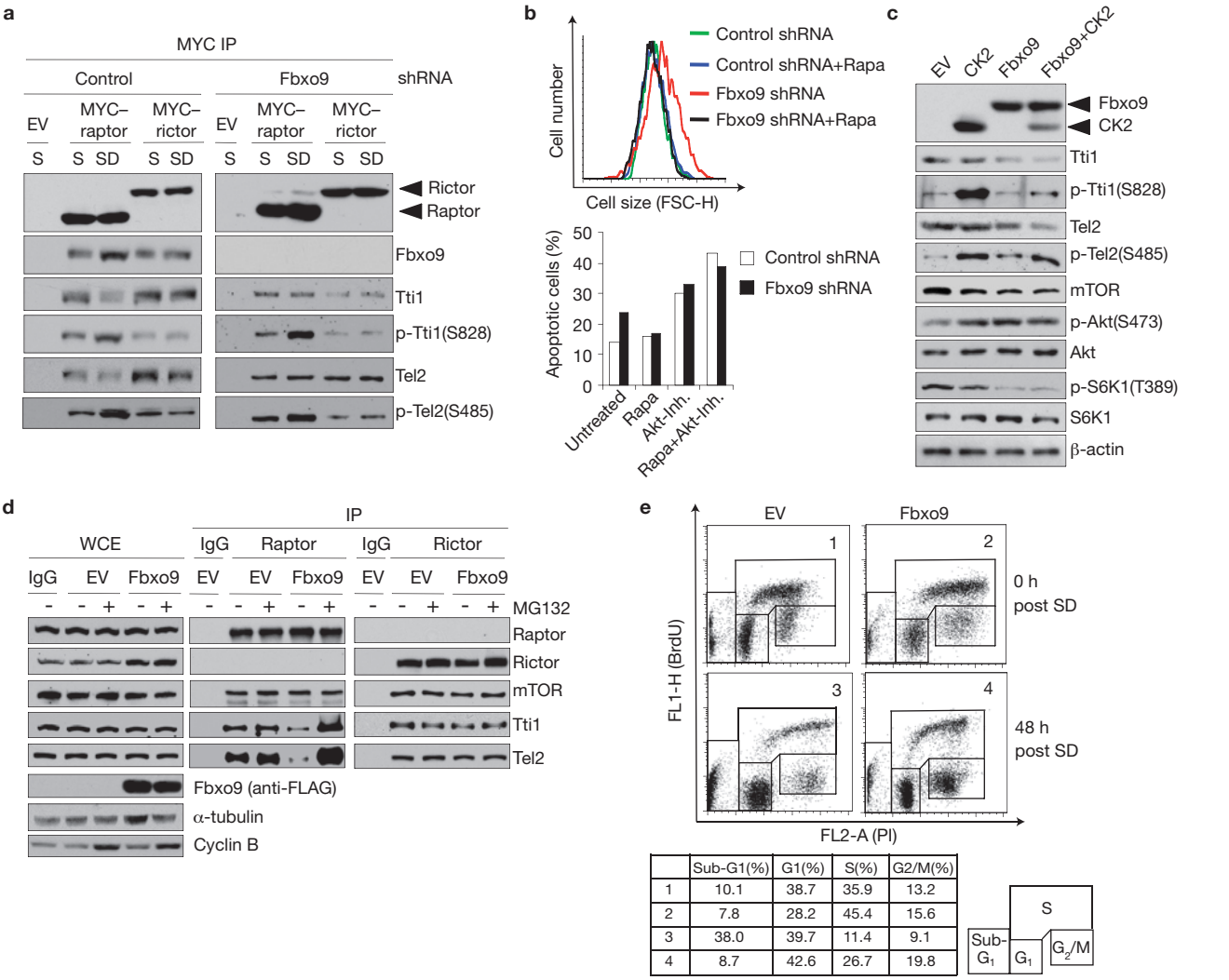

	Sub-G1(%)	G1(%)	S(%)	G2/M(%)
1	10.1	38.7	35.9	13.2
2	7.8	28.2	45.4	15.6
3	38.0	39.7	11.4	9.1
4	8.7	42.6	26.7	19.8

Figure 5 Fbxo9 preferentially targets mTORC1-bound Tel2/Tti1, thereby activating mTORC2 signalling. (**a**) HEK293T cells were transfected with empty vector (EV) or plasmids encoding MYC–raptor or MYC–rictor, serum starved (SD: 0.1% FBS) for 48 h or left untreated (S), and subjected to anti-MYC immunoprecipitations (IP). Bound protein fractions were analysed by immunoblotting for the indicated proteins. (**b**) T98G cells expressing either control or Fbxo9 shRNA were serum starved for 48 h in the presence of vehicle or rapamycin and Akt-inhibitor IV, as specified. Cells were then subjected to forward scatter analyses of G1-phase gated cells to determine cell size (upper panel) or fluorescence-activated cell sorting analyses (PI) to determine apoptosis (lower panel; $n = 2$). (**c**) HEK293T cells were transfected with empty vector or plasmids encoding CK2α and Fbxo9 as indicated. Whole-cell extracts were analysed by immunoblotting. (**d**) HEK293T cells were transfected with FLAG-tagged Fbxo9 or empty vector and treated with MG132 where indicated. Endogenous raptor and rictor were immunoprecipitated from whole-cell extracts (WCE), and immunocomplexes were probed with antibodies against the indicated proteins. (**e**) U2OS cells were treated to express FLAG-tagged Fbxo9 from retroviral transduction, fixed at the indicated time points post serum withdrawal and subjected to two-dimensional cell-cycle analysis (BrdU/PI). Uncropped images of blots/gels are shown in Supplementary Fig. S9.

CK2 derived from untreated or serum-deprived cells (Supplementary Fig. S6c). Thus, we investigated the possibility that CK2 is regulated on the level of subcellular localization. As expected, CK2 was initially mostly localized to the nucleus; however, following serum withdrawal, it substantially moved to the cytoplasm and co-localized with both Tel2 and Tti1 (Fig. 4b,c). Likewise, binding of CK2 to Tel2 and Tti1 was enhanced under serum-deprived conditions (Fig. 4d). We next generated phospho-specific antibodies against p-Tel2(S485) and p-Tti1(S828) and identified CK2-dependent phosphorylation of Tel2 and Tti1 at the Fbxo9-specific degrons in response to serum withdrawal (Fig. 4e). Moreover, knockdown of CK2 stabilized Tel2, Tti1 and mTOR, increased the level of S6K1 phosphorylation and decreased the level of Akt phosphorylation in serum-starved cells (Fig. 4f). In a reciprocal experiment, pharmacological activation of CK2 destabilized Tel2/Tti1 (Fig. 4g). These results suggest that CK2 phosphorylates Tel2 and Tti1 on serum withdrawal to mark both proteins for Fbxo9-mediated degradation, thereby inactivating mTORC1 while conserving mTORC2 signalling. A phospho-mimic mutant of Tel2 ($Tel2^{S485D}$) demonstrated cytoplasmic localization (Fig. 4h,i). Thus, whereas Tti1 is constitutively localized to the cytoplasm (Supplementary Fig. S3d), phosphorylation conserves the cytoplasmic localization of Tel2.

Fbxo9 preferentially targets mTORC1-bound Tel2/Tti1, thereby activating mTORC2 signalling

Given the differential effect of Fbxo9 on both mTORCs, we reasoned that Fbxo9 preferentially targets mTORC1-bound Tel2/Tti1 leading

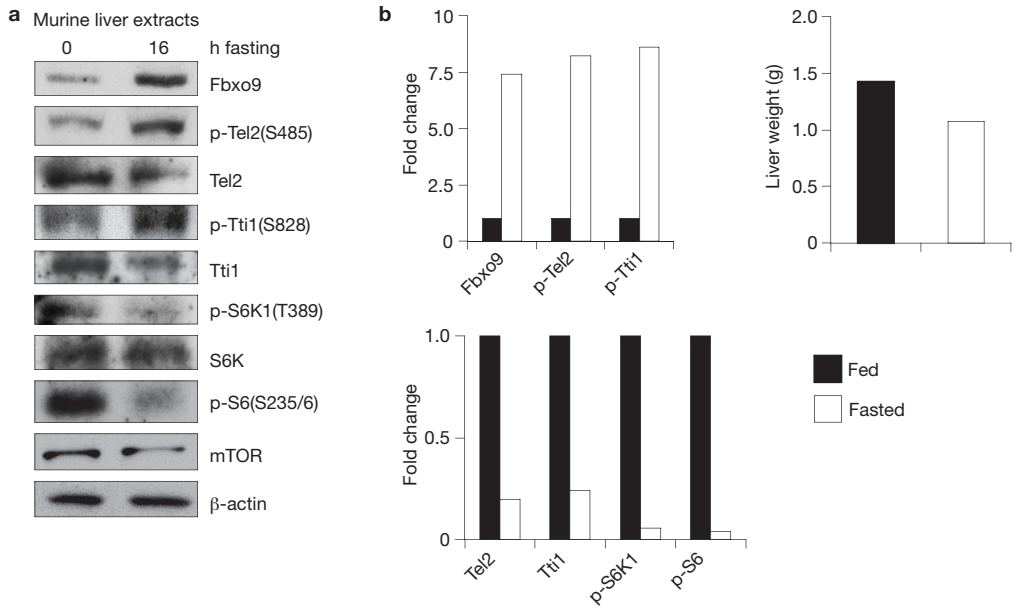

Figure 6 Starvation increases the levels of Fbxo9 expression and Tel2/Tti1 phosphorylation, but decreases Tel2/Tti1 stability and mTORC1 activity in murine liver extracts. (**a**) Wild-type C57BL/6 mice were fed or fasted for the indicated times and killed. Thereafter, liver extracts were prepared and subjected to immunoblotting using the specified antibodies. (**b**) The left panels quantify protein levels and phosphorylation shown in **a** averaged with an additional experiment ($n = 2$). The right panel quantifies liver weights of sacrificed mice ($n = 2$). The values present in the fed samples were set as 1. Uncropped images of blots/gels are shown in Supplementary Fig. S9.

to its inactivation, which in turn, activates the PI(3)K/mTORC2/Akt axis by relieving feedback inhibition[3]. In starting to investigate this possibility, we analysed Tel2/Tti1 bound to either raptor (specific for mTORC1) or rictor (specific for mTORC2) in serum-starved cells on deletion of Fbxo9. Indeed, we observed degron-specific phosphorylation and Fbxo9-dependent degradation of Tel2 and Tti1 only within mTORC1, whereas the mTORC2-associated fraction of Tel2/Tti1 remained unaffected (Fig. 5a). Likewise, Fbxo9 specifically bound raptor (and not rictor) in response to serum withdrawal (Supplementary Fig. S7a). In a complementary approach, the mTORC1-specific inhibitor rapamycin counteracted the increase in cell size and apoptosis level observed on Fbxo9 depletion, whereas combination of rapamycin with an Akt inhibitor restored the apoptosis phenotype (Fig. 5b). Finally, we performed time-course experiments to investigate whether Fbxo9- and CK2-mediated degradation of Tel2/Tti1 contributes to the immediate response to growth factor withdrawal or functions to maintain the response. Whereas a decrease in S6K1 phosphorylation was observed within 30 min, Tel2/Tti1 (within mTORC1) became unstable within 3 h post serum withdrawal (Supplementary Fig. S7b,c). These data suggest that degradation of Tel2/Tti1 via Fbxo9 and CK2 maintains the response to establish a stable state of low mTORC1 and sustained TORC2 activity.

We next analysed the effects of forced Fbxo9 overexpression, as upregulation of the PI(3)K/mTORC2/Akt pathway is commonly observed in malignancies. Forced Fbxo9 expression led to a decrease in Tel2/Tti1 levels and inhibited phosphorylation of S6K1, indicative of impaired mTORC1 signalling, and an increased Akt phosphorylation level, indicating activation of the PI(3)K/mTORC2/Akt axis. The effect was substantially enhanced when CK2 was co-expressed (Fig. 5c). This finding is in line with the reverse effect observed when either depleting Fbxo9 or expressing the stable Tti1^{S828A} mutant (Figs 1b and 3a). Next, we investigated whether forced expression of Fbxo9 leads to constitutive mTORC1-specific degradation of Tel2/Tti1, in analogy to the physiological function of Fbxo9 on growth factor withdrawal described above. Indeed, Fbxo9 expression led to a decrease in the amount of raptor-bound Tel2/Tti1, whereas the levels of rictor-bound Tel2/Tti1 remained largely unaffected. This effect was reversible on proteasome inhibition, indicating degradation of mTORC1-bound Tel2/Tti1 (Fig. 5d). Likewise, overexpression of Fbxo9 resulted in an increase in proliferation and survival levels, thus confirming sustained mTORC2 activity (Fig. 5e). These data indicate that forced expression of Fbxo9 drives mTOR signalling towards constitutive activation of the PI(3)K/mTORC2/Akt axis through the inactivation of mTORC1 and sustained loss of feedback inhibition.

Finally, we verified our data in an *in vivo* setting using liver extracts from fed or fasted mice. Extracts from fasted mice demonstrated an elevated Fbxo9 expression level and an increased level of phosphorylation of Tel2/Tti1 at the Fbxo9-specific phospho-degrons, whereas the expression level of Tel2/Tti1 and the signalling activity of mTORC1 were attenuated (Fig. 6a,b).

Fbxo9 is overexpressed in MM to promote survival

Previous array studies and Oncomine database analyses suggest overexpression and copy number gains of Fbxo9 in human MM (Supplementary Fig. S8; refs 16,22–24). Moreover, PI(3)K activation through mTORC1 inhibition has been demonstrated for deptor in a subset of MM, and Grb10, a PI(3)K inhibitor activated by mTORC1, was found to be downregulated[25–27]. We thus further investigated the role of Fbxo9 in MM. First, we measured Fbxo9 mRNA expression in 180 human MM samples. These analyses revealed an expression range covering five logarithmic ranks and overexpression of Fbxo9 (greater than fivefold compared with normal plasma cells) in 30% (54/180) of the investigated cases (Fig. 7a). There are two more or less mutually exclusive oncogenic pathways in the early development of clonal plasma

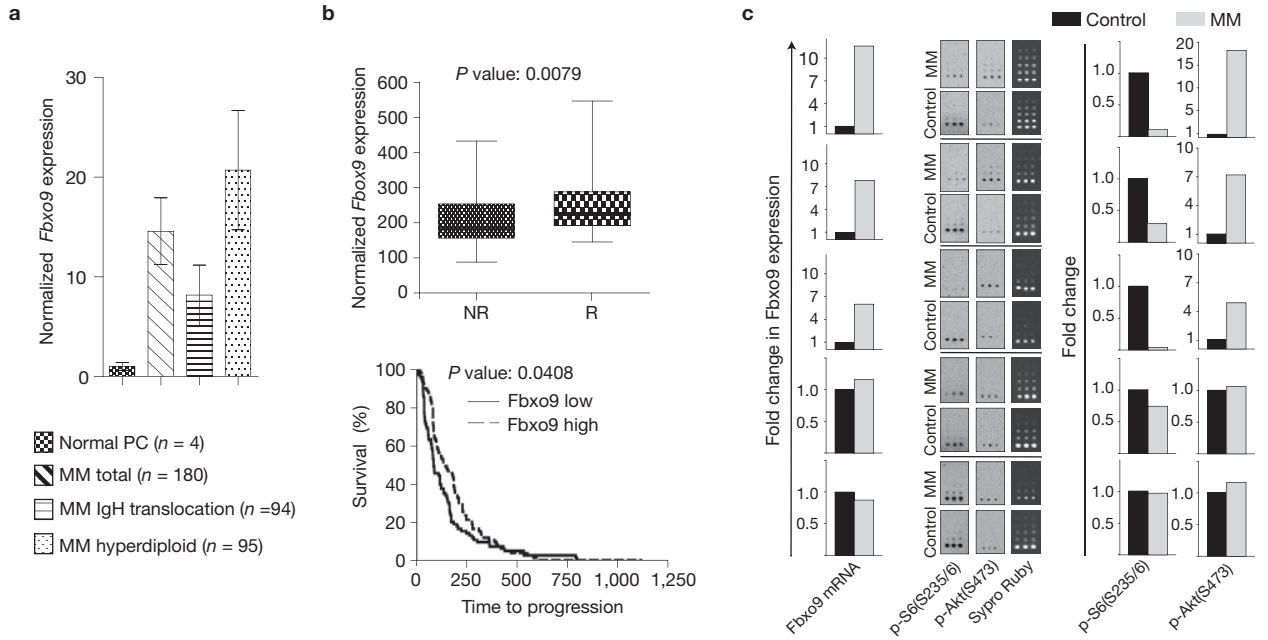

Figure 7 Analyses of Fbxo9 in primary MM patient samples. (**a**) Relative *Fbxo9* mRNA expression levels in 180 MM samples. Expression levels are normalized to the expression levels of normal plasma cells of four independent healthy donors. Of the 180 cases, 54 (30%) show an at least fivefold increased expression level compared with normal plasma cells. MM samples presenting with a hyperdiploid chromosome set express *Fbxo9* at significantly higher levels as compared with cases with a translocation involving the IgH locus. The mean *Fbxo9* expression levels are shown for each group ($n = 180$; $p = 0.03$; unpaired t-test). Error bars represent s.e.m. (**b**) Upper panel, normalized *Fbxo9* fluorescence intensities for bortezomib non-responders (NR) and responders (R). *Fbxo9* expression levels were significantly higher in R versus NR ($n = 163$; $p = 0.0079$, unpaired t-test). Box-and-whisker plots show the upper and lower quartiles (25–75%) with a line at the median; whiskers extend from the minimal to the maximal value. Lower panel, Kaplan–Meier analyses for PFS based on *Fbxo9* expression (data dichotomized at the median *Fbxo9* expression level; $n = 182$; $p = 0.041$, log-rank test). Gene expression data for this figure were derived from ref. 28. (**c**) Protein extracts were prepared from bone marrow biopsies of different MM cases and subjected to a reverse-phase protein microarray using the indicated validated antibodies.

cell disorders. Approximately half of the tumours are non-hyperdiploid and carry translocations of the immunoglobulin heavy-chain (IgH) locus and various oncogenes (for example, cyclin D1 and FGFR3). The hyperdiploid tumours exhibit recurrent trisomies, but infrequently exhibit IgH translocations[16]. Interestingly, patients harbouring a hyperdiploid chromosome set express Fbxo9 at a significantly higher level than patients with an IgH translocation (Fig. 7a). In addition, we analysed a previously published gene expression data set and found that high Fbxo9 expression levels correlate with better response and higher progression-free survival (PFS) in patients treated with the proteasome inhibitor bortezomib, supporting the notion that Fbxo9 promotes survival of MM cells in these cases[28] (Fig. 7b). Indeed, reverse-phase protein microarray analyses using extracts from MM patient bone marrow samples revealed a correlation of high levels of Fbxo9 expression with low levels of phosphorylation of S6 and high levels of phosphorylation of Akt, indicating a role for Fbxo9 in the activation of Akt in MM (Fig. 7c).

Next, we investigated different MM cell lines and found that lines with high levels of Fbxo9 exhibited low levels of expression of Tel2/Tti1 and mTOR, high levels of phosphorylation of Akt and low levels of phosphorylation of S6K1 (Fig. 8a,b), in line with our overexpression results (Fig. 5c,d). We therefore investigated whether the Fbxo9–Tel2/Tti1–mTOR axis controls survival of MM cells. Inactivation of Fbxo9 strongly induced apoptosis in MM cells with high levels of Fbxo9 expression (RPMI 8226), whereas the effect was moderate in cells with low levels of expression (U266; Fig. 8c). Accordingly, apoptotic RPMI 8226 cells demonstrated a decrease in the level of phosphorylation of Akt and an increase in the level of S6K1 phosphorylation, underscoring that Fbxo9 promotes survival through repression of mTORC1-mediated feedback inhibition of PI(3)K/mTORC2/Akt signalling (Fig. 8d). The possibility that elevated Fbxo9 levels in MM cells result from enhanced Akt activity was ruled out using the PI(3)K/Akt inhibitor wortmannin (Fig. 8e). Finally, we pharmacologically inhibited CK2 in different MM cell lines with high levels of Fbxo9 expression. Indeed, CK2 inhibition stabilized Tel2/Tti1 and mTOR and increased the level of S6K1 phosphorylation in these cells (Fig. 8f). Consistently, pharmacological activation of CK2 using sorbitol destabilized Tel2/Tti1 (Fig. 8g).

DISCUSSION

In this study, we show that Fbxo9 targets Tel2/Tti1 for proteasomal degradation in a CK2-dependent manner, thereby directly regulating mTOR signalling. We further demonstrate, that growth factor withdrawal is the physiological stimulus for this degradation event. Generally, this cellular context requires measures to avoid imminent cell death, as prolonged growth factor withdrawal is an established apoptotic stimulus. Critical steps include the switch to a state of nutritional saving and the activation of pro-survival pathways. The mTOR pathways are good candidates to accomplish these tasks. Indeed, mTORC1 controls protein translation and cell growth, two of the most energy-consuming cellular events, whereas mTORC2 promotes survival by activating Akt (ref. 3). Moreover, the presence of a negative feedback loop by which mTORC1 can inhibit the activation of the PI(3)K/mTORC2/Akt pathway provides a mechanism

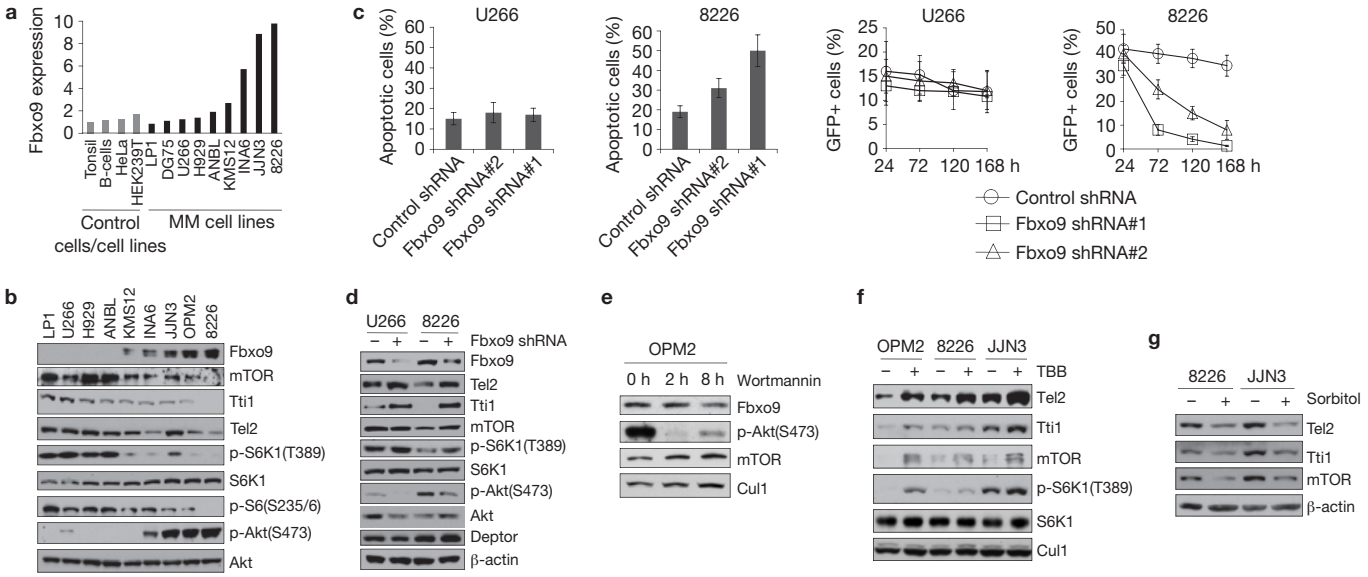

Figure 8 Fbxo9 is overexpressed in MM cells to promote survival. (**a**) Quantitative PCR analyses of Fbxo9 expression in different human MM cell lines. (**b**) Immunoblot analyses of different human MM cell lines using antibodies against the indicated proteins. (**c**) The indicated MM cell lines were lentivirally infected with shRNA constructs directed against a non-relevant mRNA or against Fbxo9 mRNA, and processed for fluorescence-activated cell sorting analyses (PI, GFP). Error bars represent s.d., $n = 3$. (**d**) Immunoblot analyses of the cells used in **c**. (**e**) OPM2 cells were treated with wortmannin for the indicated times and subjected to immunoblot analysis thereafter. (**f**) The indicated MM cell lines were treated with TBB or vehicle and probed with antibodies against the indicated proteins. (**g**) MM cell lines were treated with sorbitol as indicated and subjected to immunoblot analyses. Uncropped images of blots/gels are shown in Supplementary Fig. S9.

of how both mTORCs can be differentially regulated[3,4]. Against this background, mTORC1-specific degradation of Tel2/Tti1 provides a mechanism to minimize energy-consuming events and procure survival to avoid early cell death.

Complex specific degradation of Tel2/Tti1 may be a more general mechanism, which may provide a framework from which to address the issue of how Tel2/Tti1 can regulate the abundance of other PIKKs, which are involved in apparently disconnected signalling pathways. It would seem unlikely that all PIKKs are regulated by Tel2/Tti1 in a synchronous fashion. Notably, Tel2 and Tti1 have been shown to interact with each of the PIKKs individually[6,7,29]. It is thus tempting to speculate that PIKK-specific degradation of Tel2/Tti1 occurs in response to distinct environmental cues. In such a scenario, the identity of the involved E3 ubiquitin ligases would be of particular interest.

Another interesting finding is the identification of CK2 as the kinase, which primes Fbxo9-mediated degradation of Tel2/Tti1, particularly as CK2 is considered to be constitutively active. CK2 is involved in a multitude of cellular processes and positively regulates cell growth, proliferation and survival. Accordingly, CK2 is frequently overexpressed in various types of cancer[30,31]. However, little is known on how CK2 is regulated, and how the specificity of individual phosphorylation events is obtained in a cell-context-dependent manner[30]. Our data add spatial control (that is, nucleo-cytoplasmic translocation) as a further means to regulate CK2 in the context of serum withdrawal to support survival.

We further report overexpression of Fbxo9 in MM. This finding is intriguing, as proteasome inhibitors demonstrate high efficacy in this disease[17]. Therefore, the identification of ubiquitylation pathways whose MM-specific deregulation favours survival is critical to gain further insights into the disease. As such, we define Fbxo9- and CK2-mediated degradation of Tel2/Tti1 as a mechanism for regulating mTOR signalling. By identifying Fbxo9 overexpression as a means to constitutively activate the PI(3)K/TORC2/Akt axis in MM, we link a specific deregulated ubiquitylation event to myelomagenesis. Deptor has been shown to activate Akt by means of mTOR inhibition in certain myeloma cells[25]. Thus, deptor may contribute to the increased activity of Akt in MM as well. However, deptor was not affected by Fbxo9 and was enriched in MM cases with IgH translocations, whereas Fbxo9 is enriched in hyperdiploid MM cases[25], indicating independent pathways. We further show that a high level of Fbxo9 expression correlates with better response and higher PFS in MM patients treated with bortezomib. These data further underscore the role of Fbxo9 as a potential target in MM with a high level of Fbxo9 expression, and suggest that Fbxo9 may be a useful marker to predict clinical response to proteasomal inhibition. Likewise, inhibition of CK2 may be a complementary therapeutic approach in theses myeloma entities, particularly as CK2 inhibitors are increasingly available[32]. □

METHODS

Methods and any associated references are available in the online version of the paper.

Note: Supplementary Information is available in the online version of the paper

ACKNOWLEDGEMENTS

We thank T. deLange, T. Dechow, J. Duyster, D. Guardavaccaro, R. Humar, N. Mizushima and M. Rudelius for reagents; K. Engel and C. Proud for suggestions; R. Faessler and D. Moik for help with the antibody production; A. L. Illert for help with the preparation of liver extracts; and K-F. Becker for help with the reverse-phase protein arrays. M.P. is an investigator with the Howard Hughes Medical Institute. This work was supported by grants from the German Research Foundation (Emmy Noether Program, BA 2851/3-1) and the German Cancer Aid (#109543) to F.B.

AUTHOR CONTRIBUTIONS

V.F-S., B-S.T. and F.B. conceived and designed the research; V.F-S. and B-S.T. performed most of the experiments with crucial help from R.E., S.S., A-M.K. and

J.K.; C.L. provided the 180 MM samples, and performed cytogenetic and Fbxo9 mRNA analyses; J.S-H. provided the MM bone marrow biopsies that were processed for reverse-phase protein microarray analyses by C.R.; L.B. performed analyses of gene expression data sets; S.L. and B.K. performed mass spectrometry; M.P. provided critical reagents; V.F.S, B-S.T., R.E., S.L., C.P., M.P., B.K. and F.B. analysed results; F.B. coordinated this work and wrote the manuscript with help from V.F-S. and B-S.T. All authors discussed the results and commented on the manuscript.

COMPETING FINANCIAL INTERESTS

The authors declare no competing financial interests.

Published online at www.nature.com/doifinder/10.1038/ncb2651
Reprints and permissions information is available online at www.nature.com/reprints

1. Jorgensen, P. & Tyers, M. How cells coordinate growth and division. *Curr. Biol.* **14,** R1014–R1027 (2004).
2. Wullschleger, S., Loewith, R. & Hall, M. N. TOR signaling in growth and metabolism. *Cell* **124,** 471–484 (2006).
3. Zoncu, R., Efeyan, A. & Sabatini, D. M. mTOR: from growth signal integration to cancer, diabetes and ageing. *Nat. Rev. Mol. Cell Biol.* **12,** 21–35 (2011).
4. Mendoza, M. C., Er, E. E. & Blenis, J. The Ras-ERK and PI3K-mTOR pathways: cross-talk and compensation. *Trends Biochem. Sci.* **36,** 320–328 (2011).
5. Laplante, M. & Sabatini, D. M. mTOR signaling in growth control and disease. *Cell* **149,** 274–293 (2012).
6. Takai, H., Wang, R. C., Takai, K. K., Yang, H. & de Lange, T. Tel2 regulates the stability of PI3K-related protein kinases. *Cell* **131,** 1248–1259 (2007).
7. Hurov, K. E., Cotta-Ramusino, C. & Elledge, S. J. A genetic screen identifies the Triple T complex required for DNA damage signaling and ATM and ATR stability. *Genes Dev.* **24,** 1939–1950 (2010).
8. Takai, H., Xie, Y., de Lange, T. & Pavletich, N. P. Tel2 structure and function in the Hsp90-dependent maturation of mTOR and ATR complexes. *Genes Dev.* **24,** 2019–2030 (2010).
9. Horejsi, Z. *et al.* CK2 phospho-dependent binding of R2TP complex to TEL2 is essential for mTOR and SMG1 stability. *Mol. Cell* **39,** 839–850 (2010).
10. Kaizuka, T. *et al.* Tti1 and Tel2 are critical factors in mammalian target of rapamycin complex assembly. *J. Biol. Chem.* **285,** 20109–20116 (2010).
11. Hershko, A. & Ciechanover, A. The ubiquitin system. *Annu. Rev. Biochem.* **67,** 425–479 (1998).
12. Varshavsky, A. Three decades of studies to understand the functions of the ubiquitin family. *Methods Mol. Biol.* **832,** 1–11 (2012).
13. Bassermann, F. & Pagano, M. Dissecting the role of ubiquitylation in the DNA damage response checkpoint in G2. *Cell Death Differ.* **17,** 78–85 (2010).
14. Cardozo, T. & Pagano, M. The SCF ubiquitin ligase: insights into a molecular machine. *Nat. Rev. Mol. Cell Biol.* **5,** 739–751 (2004).
15. Skaar, J. R., D'Angiolella, V., Pagan, J. K. & Pagano, M. SnapShot: F Box Proteins II. *Cell* **137,** 1358 (2009).
16. Palumbo, A. & Anderson, K. Multiple myeloma. *New Engl. J. Med.* **364,** 1046–1060 (2011).
17. Moreau, P. *et al.* Proteasome inhibitors in multiple myeloma: 10 years later. *Blood* **120,** 947–959 (2012).
18. Rajkumar, S. V., Richardson, P. G., Hideshima, T. & Anderson, K. C. Proteasome inhibition as a novel therapeutic target in human cancer. *J. Clin. Oncol.* **23,** 630–639 (2005).
19. Busino, L. *et al.* Fbxw7α- and GSK3-mediated degradation of p100 is a pro-survival mechanism in multiple myeloma. *Nat. Cell Biol.* **14,** 375–385 (2012).
20. Bassermann, F. *et al.* The Cdc14B-Cdh1-Plk1 axis controls the G2 DNA-damage-response checkpoint. *Cell* **134,** 256–267 (2008).
21. Olsen, B. B., Guerra, B., Niefind, K. & Issinger, O. G. Structural basis of the constitutive activity of protein kinase CK2. *Methods Enzymol.* **484,** 515–529 (2010).
22. Carrasco, D. R. *et al.* High-resolution genomic profiles define distinct clinico-pathogenetic subgroups of multiple myeloma patients. *Cancer Cell* **9,** 313–325 (2006).
23. Zhan, F. *et al.* Gene-expression signature of benign monoclonal gammopathy evident in multiple myeloma is linked to good prognosis. *Blood* **109,** 1692–1700 (2007).
24. Mattioli, M. *et al.* Gene expression profiling of plasma cell dyscrasias reveals molecular patterns associated with distinct IGH translocations in multiple myeloma. *Oncogene* **24,** 2461–2473 (2005).
25. Peterson, T. R. *et al.* DEPTOR is an mTOR inhibitor frequently overexpressed in multiple myeloma cells and required for their survival. *Cell* **137,** 873–886 (2009).
26. Hsu, P. P. *et al.* The mTOR-regulated phosphoproteome reveals a mechanism of mTORC1-mediated inhibition of growth factor signaling. *Science* **332,** 1317–1322 (2011).
27. Yu, Y. *et al.* Phosphoproteomic analysis identifies Grb10 as an mTORC1 substrate that negatively regulates insulin signaling. *Science* **332,** 1322–1326 (2011).
28. Mulligan, G. *et al.* Gene expression profiling and correlation with outcome in clinical trials of the proteasome inhibitor bortezomib. *Blood* **109,** 3177–3188 (2007).
29. Rendtlew Danielsen, J. M. *et al.* HCLK2 is required for activity of the DNA damage response kinase ATR. *J. Biol. Chem.* **284,** 4140–4147 (2009).
30. Trembley, J. H., Wang, G., Unger, G., Slaton, J. & Ahmed, K. Protein kinase CK2 in health and disease: CK2: a key player in cancer biology. *Cell. Mol. Life Sci.: CMLS* **66,** 1858–1867 (2009).
31. Litchfield, D. W. Protein kinase CK2: structure, regulation and role in cellular decisions of life and death. *Biochem. J.* **369,** 1–15 (2003).
32. Battistutta, R. Protein kinase CK2 in health and disease: structural bases of protein kinase CK2 inhibition. *Cell. Mol. Life Sci.: CMLS* **66,** 1868–1889 (2009).

DOI: 10.1038/ncb2651

METHODS

Antibodies, immunoprecipitation and immunoblotting. All antibodies were used at a dilution of 1:1,000 unless specified otherwise. Mouse monoclonal antibodies were from Invitrogen (Cul1-2H4C9, 1:500, #71-8700), Sigma (β-actin-AC-74, 1:10,000, #A5316; α/β-tubulin-GTU-88, 1:5000, #T5326), Covance (HA-16B12, #MMS-101P), Biomol (ubiquitin–FK2, 1:500, #BML-PW 8810), BD Biosciences (cyclin D1-DCS-6, #556470) and Santa Cruz (Tti1-H-1, #Sc-271638). Rabbit polyclonal antibodies were from Cell Signaling (mTOR, #2972; p27, 1:200, #554069; ATM, #2873; ATR, #2790; TRRAP, #3966; S6K1, #9202; phospho-S6K1, #9234S; phospho-S6, #2211S; Akt, #4685; phospho-Akt, #9272; CK2, #2656S; cyclin B, #4138S; phospho-Chk2, #2666S; caspase-3, #8G10; cleaved caspase-3, #5A1E), Santa Cruz (HA, #Sc-805; PARP, #Sc-7150; MYC, #Sc-40), Bethyl (SMG1, #A300-393A; raptor, #A300-553A; rictor, #A300-458A), ThermoScientific (DNA-PKcs, #MS-423-PO), Novus (deptor, #NBP1-49674) and ProteinTech (Tel2, #15975-1-AP). The rabbit polyclonal antibody against Tti1 was a gift from N. Mizushima (Department of Physiology and Cell Biology, Tokyo Medical and Dental University, Japan). A polyclonal antibody against Fbxo9 was generated by immunizing rabbits with a peptide containing amino acids 390–404 of human Fbxo9. Polyclonal antibodies against p-Tel2(S485) and p-Tti1(S828) were generated with Innovagen. Extract preparation, immunoprecipitation and immunoblotting were previously described[20,31,33].

Metabolic labelling. Cell labelling with [^{35}S]Met/Cys was essentially performed as described previously[34]. Briefly, cells were washed three times with methionine- and cysteine-free DMEM and incubated with 8 ml labelling medium (Met/Cys-free DMEM, 10% dialysed fetal bovine serum (FBS) and 2 mM L-glutamine) supplemented with 0.2 mCi ml^{-1} of [^{35}S]Met/Cys mix for 2 h.

***In vivo* protein translation assay.** HEK293T cells were seeded in a 24-well plate and transfected with either pcDNA3.1 Tti1 (wild type or mutant) or short interfering RNA (siRNA) oligonucleotides directed against Fbxo9 or LacZ, a 5′ structured stem–loop luciferase reporter gene (pcDNA-SL-LUC; ref. 35) and a pRL-null *Renilla* luciferase plasmid. The luciferase activity was measured using a dual-luciferase reporter assay system (Promega).

***In vitro* kinase assay.** Active CK2 and purified substrates (FLAG-tagged forms of Tel2 wild type, Tel2$^{S485/487A}$, Tel2^{S485A}, Tti1 wild type and Tti1^{S828A}) were transferred into the kinase reactions that contained 80 mM HEPES, at pH 7.4, 10 mM $MgCl_2$, 50 μM ATP, 1 μCi [γ−^{32}P]ATP (Hartmann Analytic) and 1 mM dithiothreitol. The kinase reaction was carried out at 30 °C for 10 min as previously described[36].

Cell culture and drug treatment. U2OS cells were cultured in McCoy's 5A medium, and HEK293T, HeLa, IMR90 and T98G cells were cultured in Dulbecco's modified Eagle's medium (DMEM), with each medium containing 10% FBS. Human T98G cells are revertants from T98 glioblastoma cells that acquired the property to arrest efficiently in G0/1 phase in low serum[20,37,38]. The MM cell lines U266, KMS12, RPMI 8226, DG75, H929, ANBL, JJN3, LP1 and OPM2 were cultured in RPMI-1640 with 10% FBS. INA-6 cells were supplemented with 5 ng ml^{-1} IL-6. Where indicated, the following drugs were used: MG132 (10 μM), wortmannin (500 nM), rapamycin at (50 nM), Akt inhibitor IV (5 μM), TBB (50 μM) and sorbitol (500 mM).

Murine liver extracts. Male wild-type C57BL/6 mice were fed or fasted for 16 h. After the mice were killed, their livers were weighed and perfused with an EDTA-containing buffer. Hepatocytes were isolated essentially as described previously[39]. Experiments were performed in accordance with the local ethical guidelines.

Recombinant proteins. Complementary DNAs encoding the entire coding region of human Fbxo9, Fbxw7, Cul1, Roc1 and Skp1 were inserted into the baculoviral expression vector pFastBac HTb (Invitrogen). Recombinant proteins were produced in 5B insect cells as described previously[34,40]. Tel2 and Tti1 proteins were purified from HEK293T cells via FLAG immunoprecipitation followed by FLAG–peptide elution and dialysis against PBS. GST fusion proteins were generated as described previously[20].

***In vitro* ubiquitylation assay.** The ubiquitylation of Tel2 and Tti1 was performed in a volume of 10 μl containing 50 mM Tris at pH 7.6, 5 mM $MgCl_2$, 0.6 mM dithiothreitol, 2 mM ATP, 1.5 ng μl^{-1} E1 (Boston Biochem), 10 ng μl^{-1} Ubc3, 10 ng μl^{-1} Ubc5, 2.5 μg μl^{-1} ubiquitin (Sigma), 1 μM ubiquitin aldehyde, 2 μl of purified Tel2 or Tti1 proteins, and approximately 500 ng each of purified Skp1^{Fbxo9} or Skp1^{Fbxw7} together with Cul1–Roc1 complexes.

Transient transfections, retrovirus and lentivirus-mediated DNA transfer. HEK293T cells were transfected using the calcium phosphate method[5]. For retrovirus production, GP-293 packaging cells (Clontech) were transfected with Lipofectamine transfection reagent (Invitrogen). At 48 h post transfection, the virus-containing medium was collected and supplemented with 8 μg ml^{-1} Polybrene (Sigma).

Cell-cycle analysis. For BrdU incorporation and DNA content analysis, cells were pulsed with 10 μM BrdU (Sigma) for 1 h and stained using a standard protocol. Two-dimensional flow cytometry was performed to detect FITC and PI as described previously[6,7]. For quantification, FlowJo software (Tree Star) was used.

Immunofluorescence microscopy. Immunofluorescence microscopy was performed as described previously[7]. Images were taken using the laser-scanning confocal microscope FluoView FV10i (Olympus). For quantification, 100 cells for each condition were analysed in three sets.

Purification of Fbxo9 interactors and phospho-analyses of Tel2 and Tti1. About 2 × 10^9 HEK293T cells were transfected with an Fbxo9-tandem-Strep-single-FLAG-tagged (Fbxo9-SF-TAP) construct or SF-TAP empty vector[3] as described previously[4]. Fbxo9 was precipitated with streptactin superflow resin (IBA). After washing, Fbxo9-interacting proteins were eluted twice using desthiobiotin elution buffer (IBA). The eluate was then subjected to a second precipitation with anti-FLAG resin (anti-FLAG-M2-agarose; Sigma) and then subjected to a further competition with FLAG peptide (Sigma). Peptides generated by in-gel trypsin digestion were dried and dissolved in 0.1% formic acid. Liquid chromatography with tandem mass spectrometry was performed by coupling a nanoLC-Ultra (Eksigent) to a LTQ Orbitrap XL mass spectrometer (ThermoFisher Scientific), using a 60 min gradient from 0 to 40% solution B (0.1% formic acid in acetonitrile).

For phosphorylation analyses, Tel2 and Tti1 were immunoprecipitated with anti-FLAG resin and eluted twice by competition with FLAG peptide. Gel bands containing Tel2 or Tti were cut out and in-gel trypsin digestion was performed. PHOS-Select (Sigma) iron-coated beads were mixed with the peptide mixture and incubated for 30 min at room temperature. Phosphopeptides were directly eluted onto a stainless-steel matrix-assisted laser desorption/ionization (MALDI) target (Bruker Daltonik). Mass spectra were acquired in positive-ion reflectron mode on an ultrafleXtreme MALDI tandem time-of-flight mass spectrometer equipped with a 1 kHz Smartbeam-II laser (Bruker Daltonik). Tandem mass spectra were acquired in positive-ion reflectron mode using the LIFT technique with an increased laser intensity (+40%).

mRNA expression in cell lines. For quantification of Fbxo9, mTOR, Tel2, Tti1 18S rRNA and GAPDH mRNA expression levels, total RNA was extracted using the RNeasy Kit (Qiagen). cDNA synthesis was performed using Superscript III (Invitrogen). Quantitative PCR analysis (SYBR green) was performed according to standard procedures. Primer sequences were: *Fbxo9*: 5′-GGGCAACTGGTGTGTTTATATGCC-3′ and 5′-TGTGCCTGCAGATCTGTTTCAGC-3′; *GAPDH*: 5′-GAAGGTGAAGGTCGGAGTC-3′ and 5′-GAAGATGGTGATGGGATTTC-3′; *18S rRNA*: 5′-GCACTGGAAGTCCAACTACTTC-3′ and 5′-TGAGGTCCTCCTTGGTGAACAC-3′; *Tel2*: 5′-TGGAGGTGCCCAAGATTACCTG-3′ and 5′-CCTTGCCCATGGCCACAG-3′; *Tti1*: 5′-TGCTCTGATGGCAGCATTAGCC-3′ and 5′-TGGAGGTGCCCAAGATTACCTG-3′; *mTOR*: 5′-CTGGGACTCAAATGTGTGCAGTTC-3′ and 5′-GAACAATAGGGTGAATGATCCGGG-3′.

Fbxo9 mRNA expression and cytogenetic analyses in MM patient samples. Fbxo9 mRNA expression was measured by quantitative real-time PCR with reverse transcription (RT–PCR; SYBR green) from CD138-purified plasma cells from 180 patients with MM archived at the Department of Hematology/Oncology, University of Ulm, Germany. Total RNA extraction and cDNA synthesis were performed according to standard procedures. Fbxo9 mRNA expression was normalized to *18S rRNA* and calculated using the 2-ΔΔCT method. All patients were characterized by a comprehensive set of fluorescence *in situ* hybridization probes for the presence of recurring cytogenetic abnormalities.

Extract preparation of formalin-fixed bone marrow biopsies and reverse-phase protein lysate microarrays. Formalin-fixed bone marrow biopsies of MM patients (>70% infiltration) were selected from the archive of the Institute of Pathology, Technische Universität München, Germany. Extract preparation was performed as described previously[41]. Protein arrays were generated using the Calligrapher MiniArrayer (BioRad). For every extract and every dilution (undiluted, 1:2, 1:4, 1:8, 1:16, buffer), three replicates were applied onto a nitrocellulose-coated glass slide[42] (Grace Bio-Labs). For quantification, parallel arrays were stained with Sypro Ruby (Molecular Probes).

Plasmids, shRNAs and siRNAs. cDNAs of CK2, Tel2 wild type, Tti1 wild type, Tel2/Tti1 point and deletion mutants, Fbxo9, Fbxo3, Fbxo4, Fbxo11 and

Fbxo18 were cloned into pcDNA 3.1 or pcDNA-N-SF-TAP, respectively. For retrovirus production, Fbxo9, Tel2 wild type, Tti1 wild type and Tel2/Tti1 point and deletion mutants were subcloned into the retroviral vectors pMSCV and/or pLPC. MYC–raptor and MYC–rictor were a gift from D. Sabatini (Whitehead Institute, MIT, USA; Addgene plasmids 11367 and 1859, respectively). All cDNAs were sequenced. For shRNA-mediated silencing of Fbxo9, SMARTvector 2.0 lentiviral shRNA particles (Dharmacon) were used. The target sequences for human Fbxo9 were: (#1) 5′-GTATTAACTTGTTCCGTA-3′; (#2) 5′-AACCACATATATTCGTCA-3′; (#3) 5′-TTATACTCCTCTTTACGCA-3′. For siRNA-mediated silencing, duplexes were purchased from Dharmacon and transfected into subconfluent cells using HiPerfect reagent (Qiagen). The target sequences for human Fbxo9, Tti1, Tel2 and CK2α were: Fbxo9 (#1) 5′-GGUGUAAGCUCUAGCAAUU-3′, (#2) 5′-GUAUUAAACUUGUUCCGUA-3′, (#3) 5′-GAGCUCAGUGGAUGUUUGA-3′, (#4) 5′-GCAACUUGUACCUGAUAUA-3′; CK2α (#1) 5′-AACAUUGUCUGUACAGGUU-3′, (#2) 5′-CGUGGUCGCUUACAUCACU-3′, (#3) 5′-GGAGUGUGUCUUAGUUAC-3′', (#4) 5′-GCAUUUAGGUGGAGACUUC-3′; Tel2 (#1) 5′-GAGCGGAUCAGAAGCAAGA-3′, (#2) 5′-UGAUGUGCCUGGCUGUUAA-3′, (#3) 5′-GUACGAAGAGGAUGAACUG-3′, (#4) 5′-GAAGACCUGUGUGGUGGGA-3′; Tti1 (#1) 5′-GCACUGACCAGGCUUAUCA-3′, (#2) 5′-AGGAUUUGCUGUAUCUUUA-3′, (#3) 5′-GUGAAUGGGAUCUCUUUAA-3′, (#4) 5′-GAACACACCUGCCAAGUUA-3′. A LacZ siRNA served as a control.

Statistical analysis. Fbxo9 mRNA expression levels in primary MM samples ($n = 180$) from quantitative RT–PCR experiments were normalized to the expression of normal plasma cells ($n = 4$). Statistical significance between cytogenetic subgroups was measured by a one-tailed unpaired t-test. The correlation between Fbxo9 expression and the response to bortezomib was analysed on a previously published gene expression data set[28]. MM samples were grouped on the basis of the median Fbxo9 expression level (probe set 238472_at). Statistical significance between bortezomib-responding and non-responding patients ($n = 163$) was tested by a two-tailed unpaired t-test. To determine whether Fbxo9 expression associates with outcome, the same data set was reanalysed. Fbxo9 expression (probe set 238472_at) was dichotomized at the median Fbxo9 expression level ($n = 182$). Estimated probabilities of PFS were calculated using the Kaplan–Meier method using GraphPad Prism 4 software, and the log-rank test evaluated differences between survival distributions. Oncomine-derived expression data were analysed by Student's t-test directly through the Oncomine 4.4.3 software (www.oncomine.org).

Referenced accession numbers. Data sets reanalysed in the study are accessible through NCBIs Gene Expression Omnibus (GEO; http://www.ncbi.nlm.nih.gov/geo/) under accession numbers GSE9782 (Fig. 7b), GSE2113, GSE2658 and GSE5900 (Supplementary Fig. S8).

33. Fernandez-Saiz, V. & Buchberger, A. Imbalances in p97 co-factor interactions in human proteinopathy. *EMBO Rep.* **11,** 479–485 (2010).
34. Bassermann, F. *et al.* NIPA defines an SCF-type mammalian E3 ligase that regulates mitotic entry. *Cell* **122,** 45–57 (2005).
35. Dorrello, N. V. *et al.* S6K1- and βTRCP-mediated degradation of PDCD4 promotes protein translation and cell growth. *Science* **314,** 467–471 (2006).
36. Bassermann, F. *et al.* Multisite phosphorylation of nuclear interaction partner of ALK (NIPA) at G2/M involves cyclin B1/Cdk1. *J. Biol. Chem.* **282,** 15965–15972 (2007).
37. Stein, G. H. T98G: an anchorage-independent human tumor cell line that exhibits stationary phase G1 arrest *in vitro*. *J. Cell Physiol.* **99,** 43–54 (1979).
38. Lisztwan, J. *et al.* Association of human CUL-1 and ubiquitin-conjugating enzyme CDC34 with the F-box protein p45(SKP2): evidence for evolutionary conservation in the subunit composition of the CDC34-SCF pathway. *EMBO J.* **17,** 368–383 (1998).
39. Meredith, M. J. Rat hepatocytes prepared without collagenase: prolonged retention of differentiated characteristics in culture. *Cell Biol. Toxicol.* **4,** 405–425 (1988).
40. Busino, L. *et al.* SCFFbxl3 controls the oscillation of the circadian clock by directing the degradation of cryptochrome proteins. *Science* **316,** 900–904 (2007).
41. Becker, K. F. *et al.* Quantitative protein analysis from formalin-fixed tissues: implications for translational clinical research and nanoscale molecular diagnosis. *J. Pathol.* **211,** 370–378 (2007).
42. Wolff, C., Schott, C., Malinowsky, K., Berg, D. & Becker, K. F. Producing reverse phase protein microarrays from formalin-fixed tissues. *Methods Mol. Biol.* **785,** 123–140 (2011).

DOI: 10.1038/ncb2651

nature cell biology

a

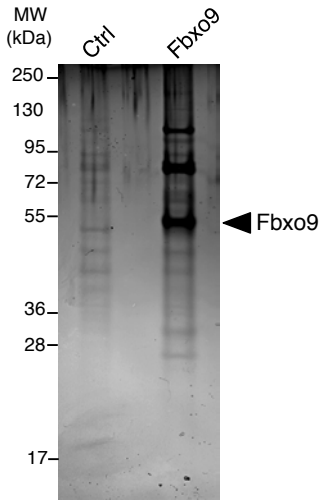

b

Telomere Length regulation protein Tel2 homolog IPI00016868

Sequence	Mascot Ion score	Modifications	Start	Stop
(R)QGLLSAVSSVLLSLPAAR(L)	72.1		768	785
(R)EVSVELAK(V)	26.45		551	558
(R)LVEQVPDR(A)	28.05		255	262
(R)QGLLSAVSSVLLSLPAAR(L)	34.48		768	785
(R)AmEAVLTGLVEAALGPEVLSR(L)	25.89	Oxidation (+16)	263	283
(R)LLEDLMDELLEAR(S)	90.83		786	798
(R)LLEDLmDELLEAR(S)	73.31	Oxidation (+16)	786	798
(K)AVLIcLAQLGEPELR(D)	63.76	Carbamidomethyl (+57)	363	377
(R)QGLLSAVSSVLLSLPAAR(L)	94.96		768	785
(R)LQQENLAEFFPQNYFR(L)	111.71		171	186
(R)AmEAVLTGLVEAALGPEVLSR(L)	90.93	Oxidation (+16)	263	283

Tel2-Interacting protein 1 homolog IPI 00011702

Sequence	Mascot Ion score	Modifications	Start	Stop
(K)FSTLSLLLGYLK(L)	41.07		398	409
(K)ALADILSESLHSLATSLPR(L)	47.69		369	387
(K)FSTLSLLLGYLK(L)	92.03		398	409
(K)ALIQVLELDVADIK(I)	76.35		431	444
(K)QLGDLFASFLPGISTALTR(L)	71.94		201	219

Figure S1 Purification of the Fbxo9 complex. **a,** Tandem-Strep-single-FLAG-tagged (SF-TAP)-Fbxo9 was expressed in HEK293 cells ($2x10^9$ cells) and subjected to a sequential immunopurification approach comprising immobilization on Strep-Tactin beads and elution with desthiobiotin in the first step, and immobilization on anti-FLAG resin and elution with 3x-FLAG-octapeptide in the second step. The FLAG eluate was separated by SDS-PAGE and analyzed by mass spectrometry. As a control, a purification was performed from HEK293 cells ($5x10^8$ cells) transfected with an empty vector. The depicted gel corresponds to 5% of the final FLAG-eluates visualized by silver staining. **b**, Sequences of identified peptides corresponding to Tel2 and Tti1.

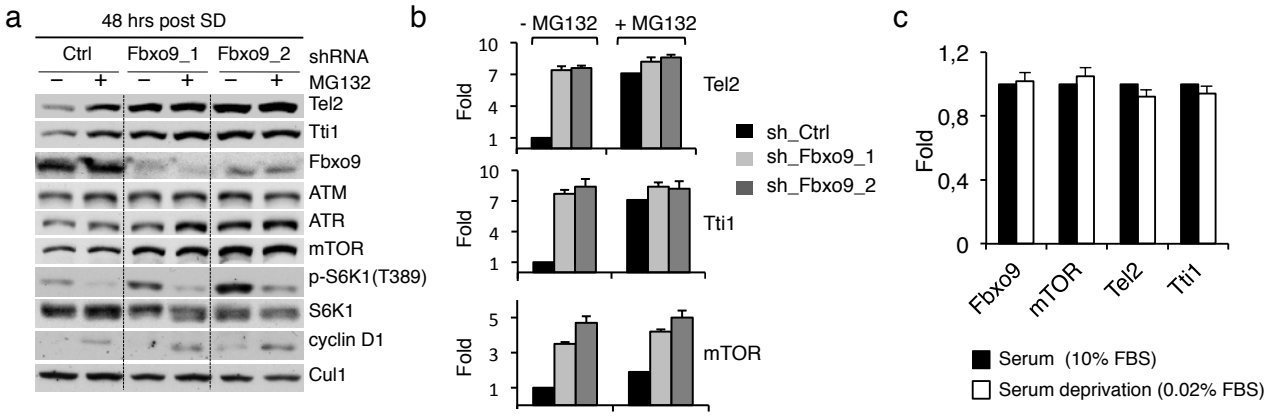

Figure S2 Fbxo9 mediates ubiquitin-proteasome dependent degradation of Tel2 and Tti1. **a,** T98G cells were infected with shRNA constructs directed against a nonrelevant mRNA or against two distinct sequences of Fbxo9 mRNA. Cells were deprived of serum (SD: 0.02% FBS) for the indicated times and during the last 4 hrs before harvesting, cells were treated with MG132 where indicated. Protein extracts were analyzed by immunoblotting with antibodies to the indicated proteins. **b**, Quantification of proteins shown in (a) averaged with two additional, independent experiments. The value given for the amount of protein present in the control sample (-MG132) was set as 1. Error bars represent s.d., n = 3. **c**, mRNA levels of the indicated genes were analyzed in serum treated or serum deprived (48hrs) T98G cells using real-time PCR. Error bars represent s.d., n = 3. The value given for the amount of mRNA in the serum treated sample of each gene was set as 1.

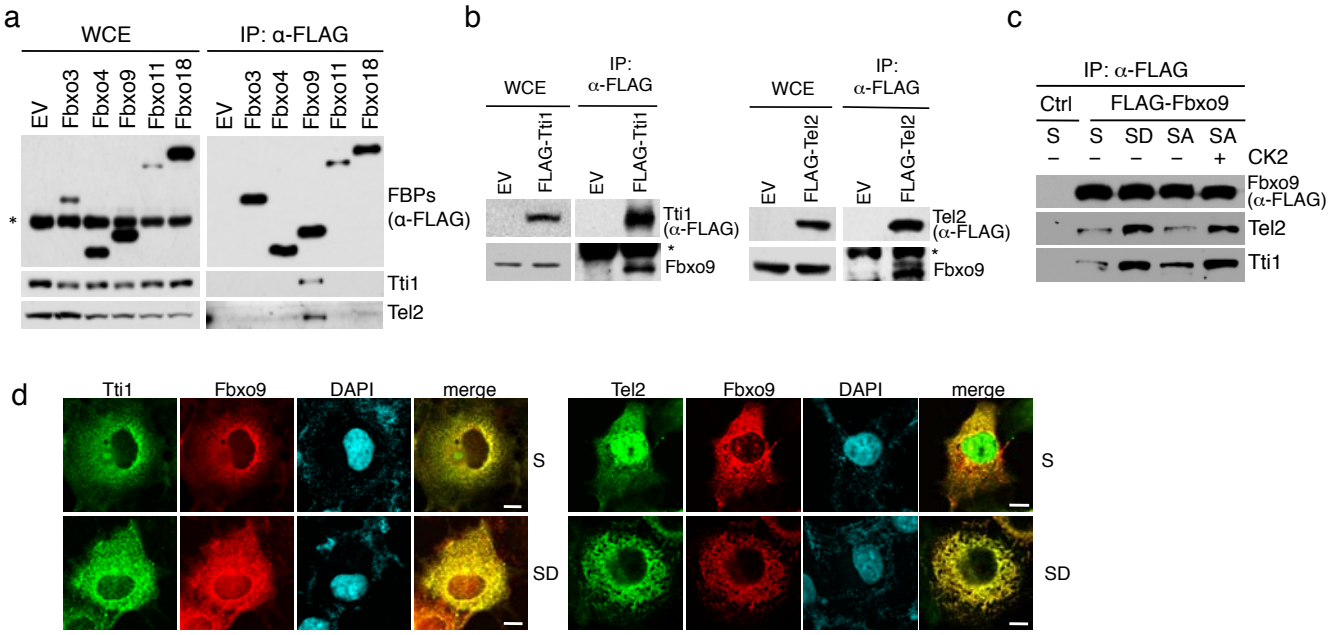

Figure S3 Fbxo9 interacts with Tel2 and Tti1 proteins. **a,** HEK293 cells were transfected with empty vector (EV) or constructs of the indicated FLAG-tagged F-box protein (FBPs). Whole cell extracts (WCE) were immunoprecipitated (IP) with anti-FLAG beads, and immunoprecipitates subsequently probed with antibodies to the indicated proteins. **b,** HEK293 cells were transfected with empty vector or FLAG-tagged Tel2 or Tti1 constructs. WCE were immunoprecipitated with anti-FLAG beads as in (**a**), and probed with the indicated antibodies. Asterisks denote nonspecific bands. **c,** U2OS cells, infected with a retrovirus expressing FLAG-tagged Fbxo9 or control virus and transfected with a CK2 expression plasmid as indicated, were either grown in normal serum (S: 10% FBS) or deprived of serum for 48 hrs (SD: 0.1% FBS) and then activated with serum for 2 hrs (SA:10% FBS). Thereafter, WCE were prepared, subjected to immunoprecipitations with anti-FLAG beads as described in (**a**), and immunoblotted with antibodies to the indicated proteins. **d,** Colocalization of Fbxo9 and Tel2/Tti1. Cos7 cells were transiently transfected with plasmids encoding HA-tagged Fbxo9 and either FLAG-tagged Tel2 or Tti1. Cells were then cultured in normal serum (S: 10% FBS) or deprived of serum for 5 hrs (SD: 0.02% FBS). Thereafter, cells were fixed with methanol and incubated with anti-FLAG antibody (green) and anti-HA antibody (red). DNA was stained with DAPI (blue). Scale bar, 10 μm.

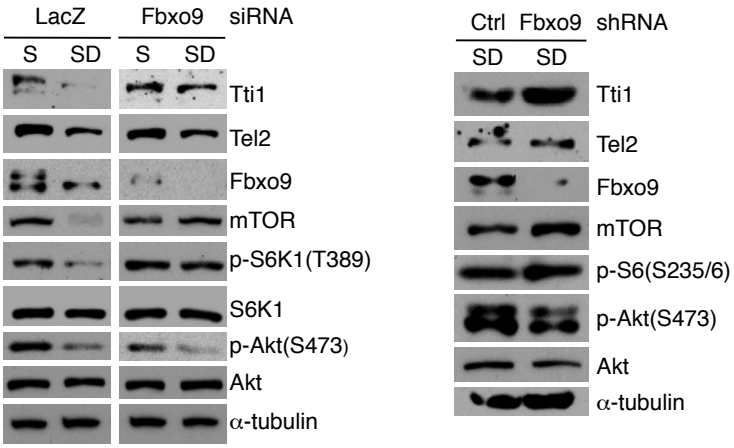

Figure S4. Fbxo9 promotes degradation of Tel2 and Tti1 proteins in response to serum withdrawal in primary IMR90 cells. IMR90 cells were treated with siRNAs directed against Fbxo9 or LacZ (left panel) or infected twice with shRNA constructs directed against Fbxo9 mRNA or against a nonrelevant mRNA (right panel). Cells were grown in normal medium (S:10% FBS) or deprived of serum (SD: 0.2% FBS) for 48 hrs. Protein extracts were then prepared and probed with antibodies as specified.

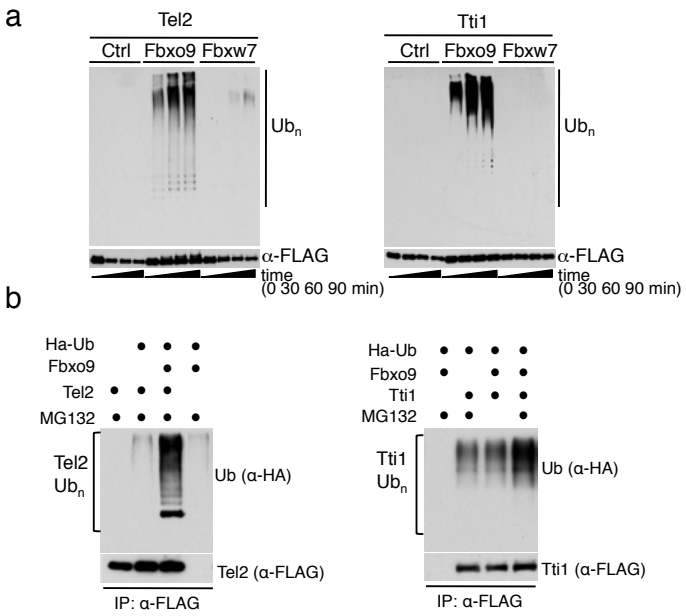

Figure S5 *In vitro* **and** *in vivo* ubiquitylation of Tel2/Tti1 proteins via Fbxo9. **a,** *In vitro* ubiquitylation assays of Tel2 and Tti1 proteins. SCF^{Fbxo9} and SCF^{Fbxw7} were expressed using baculoviruses and purified from Sf21 insect cells. FLAG-tagged Tel2 and Tti1 were immunoprecipitated from HEK293 cells. Samples were supplemented with ubiquitin, E1, and E2, incubated as specified, and subjected to immunoblotting with the indicated antibodies. The brackets on the right side mark polyubiquitylated Tel2 or Tti1. **b,** *In vivo* ubiquitylation assays of Tel2 and Tti1 proteins. HEK293 cells were transfected with plasmids expressing FLAG-tagged Tel2 or Tti1, HA-ubiquitin and Fbxo9 as indicated. Following treatment with MG132, extracts were prepared and subjected to anti-FLAG-immunoprecipitations using denaturing conditions.

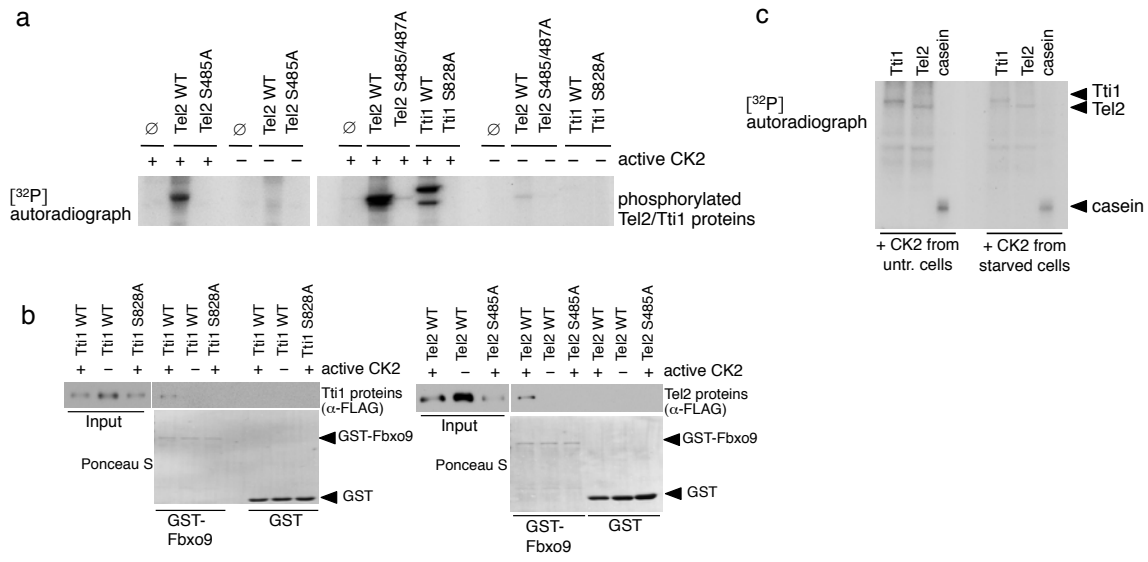

Figure S6 CK2 phosphorylates Tel2 and Tti1 proteins and mediates binding to Fbxo9 *in vitro*. **a,** Equal amounts of the indicated purified forms of Tel2 and Tti1 were transferred to an *in vitro* kinase reaction to test for phosphorylation by purified active CK2 in the presence of [^{32}P]ATP. Phosphorylated proteins were visualized by autoradiography. **b,** The indicated forms of purified Tel2 and Tti1 were phosphorylated by CK2 *in vitro* as indicated, and tested for their binding to GST-tagged Fbxo9 using *in vitro* pull-down assays. **c,** FLAG-CK2α was immunoprecipitated from untreated or serum starved cells and subjected to an an *in vitro* kinase reaction using purified Tel2, Tti1 and casein as substrates. Phosphorylated proteins were visualized by autoradiography.

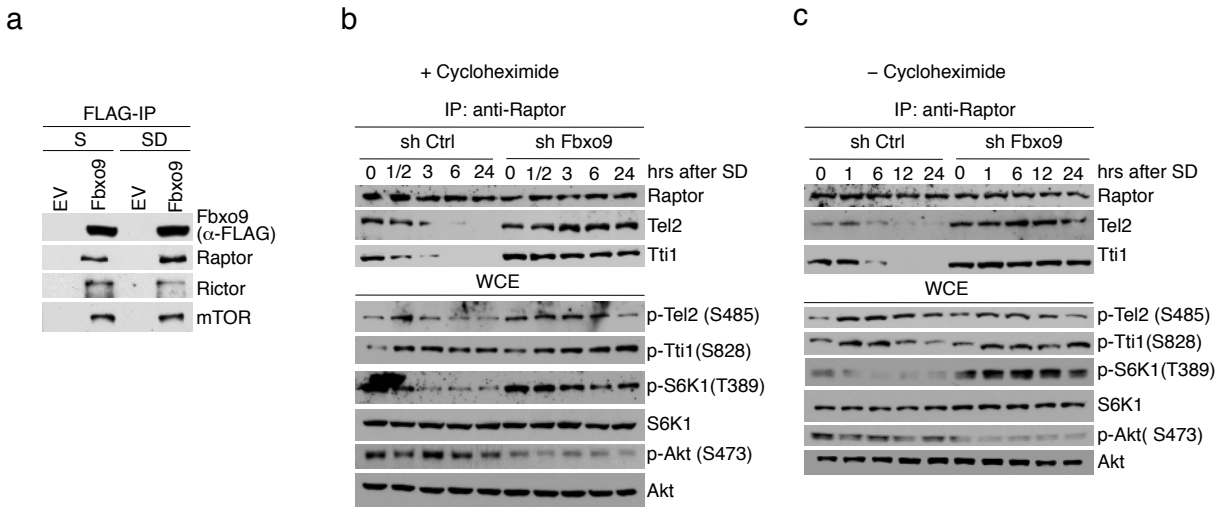

Figure S7 mTORC1 specific degradation of Tel2/Tti1 via Fbxo9 maintains the cellular response to growth factor withdrawal. **a,** T98G cells expressing FLAG-Fbxo9 from retroviral infection were grown in the presence of serum (S: 10 % FBS) or deprived of serum (SD: 0.02% FBS) for 48 hrs. Thereafter, anti-FLAG immunopreciptitations were performed and and probed with antibodies as specified. **b,** T98G cells treated to downregulate Fbxo9 or control cells were deprived of serum (SD: 0.02% FBS) in the presence of cycloheximide and harvested at the indicated timepoints. Endogenous Raptor was subsequently immunoprecipitated (IP) from whole cell extracts (WCE), and immunocomplexes and WCE were probed with antibodies to the indicated proteins. **c,** The experiment was essentially performed as in **(b)**, except that cycloheximide was omitted.

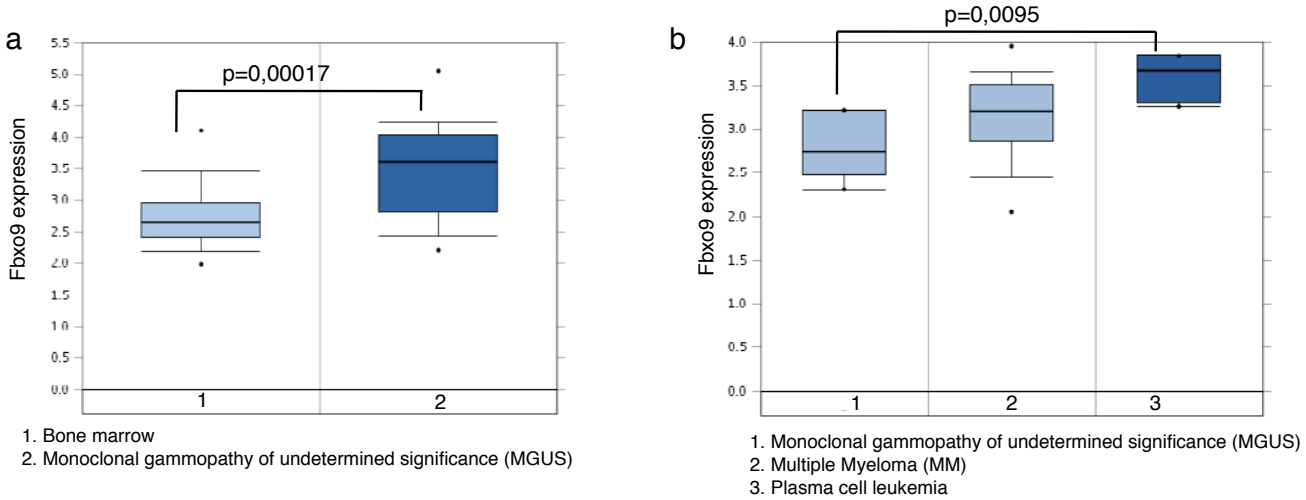

Figure S8 *Fbxo9* expression correlates with MM progression. All data was provided by the Oncomine database. The associated p values are shown for each study. **a,** Data from (23) reanalyzed to show expression levels of *Fbxo9* in normal bone marrow and monoclonal gammopathy of undetermined significance (MGUS) (n = 78). **b,** Data from (24) reanalyzed to show expression levels of *Fbxo9* in MGUS, MM, and plasma cell leukemia (n = 52). Both box-and-whisker plots show the upper and lower quartiles (25–75%) with a line at the median, whiskers extend from the 10th to the 90th percentile, and dots correspond to minimal and maximal values.

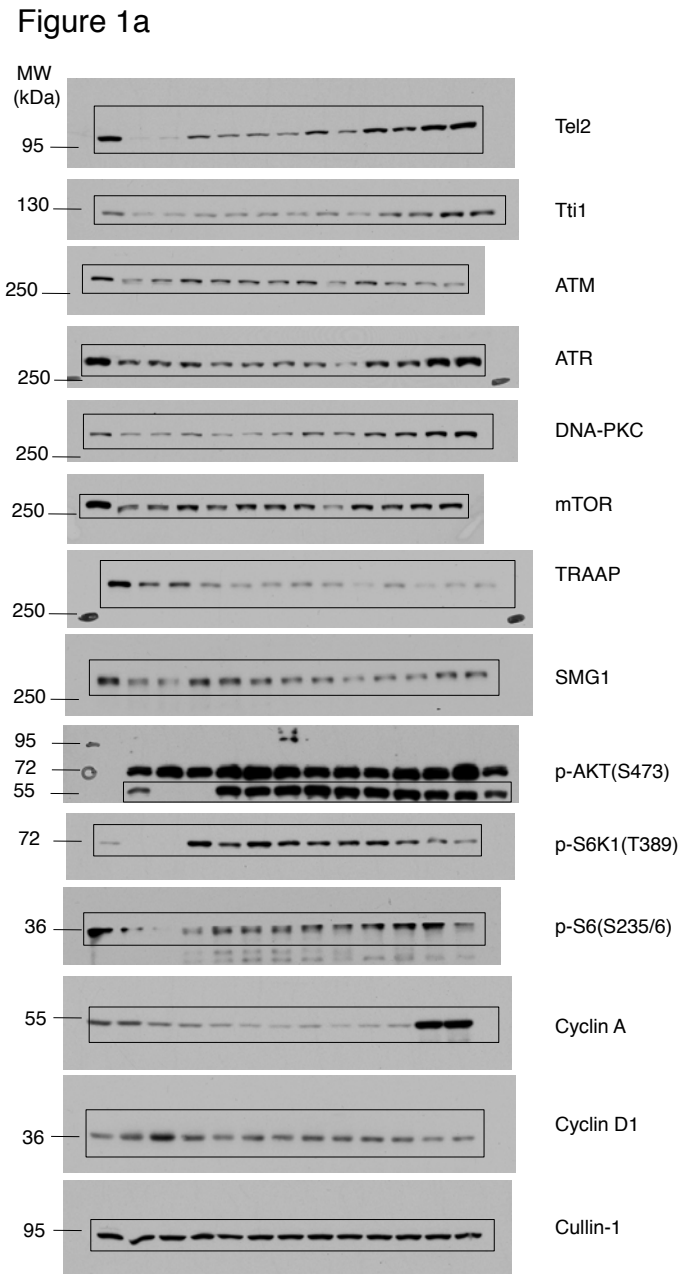

Figure S9 Full scans

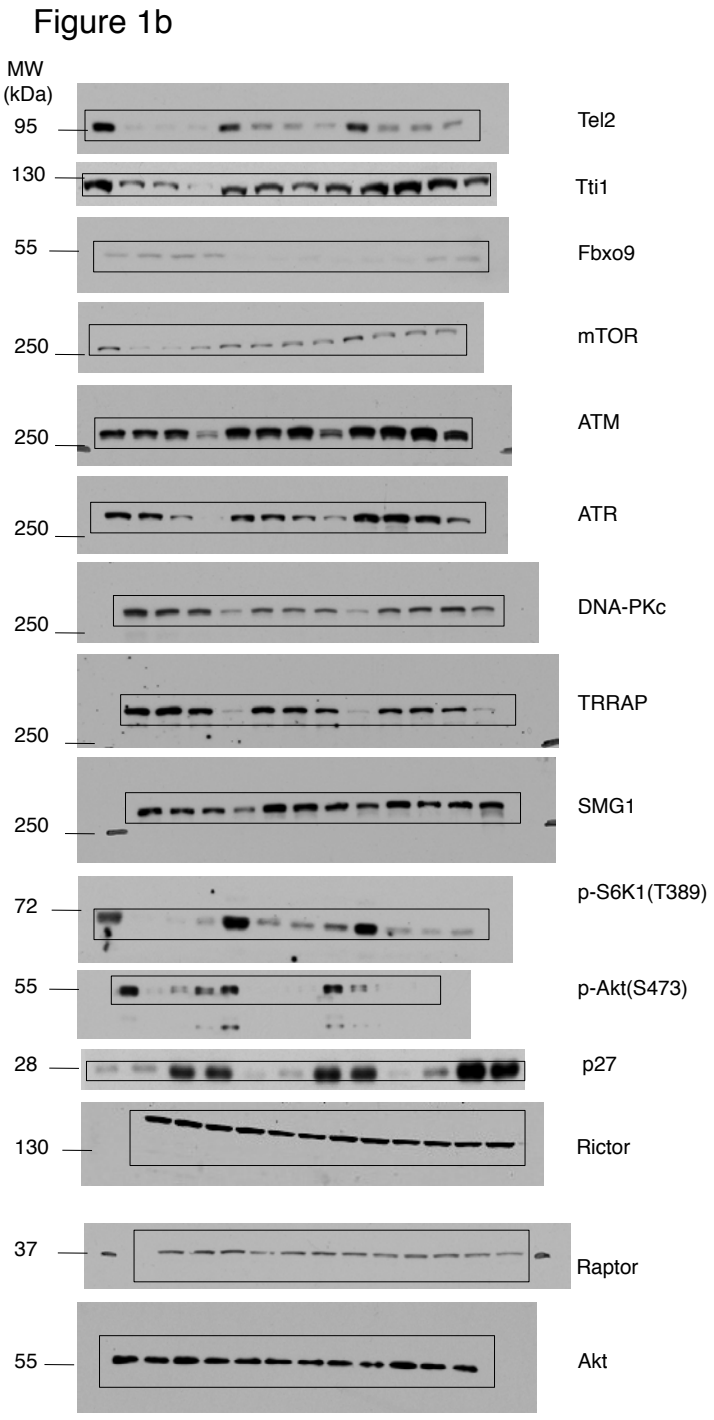

Figure S9 Full scans continued

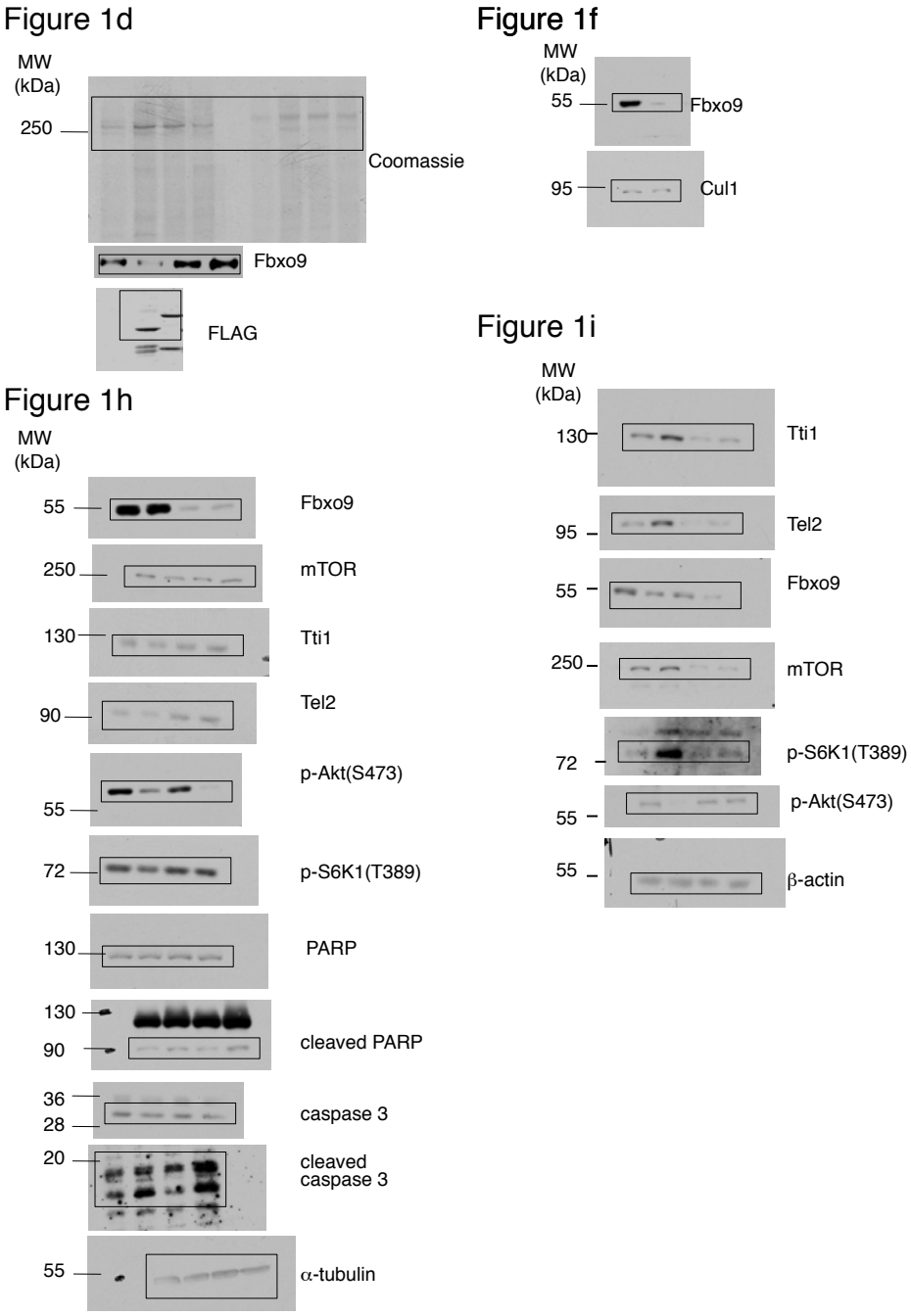

Figure S9 Full scans continued

Figure 2a

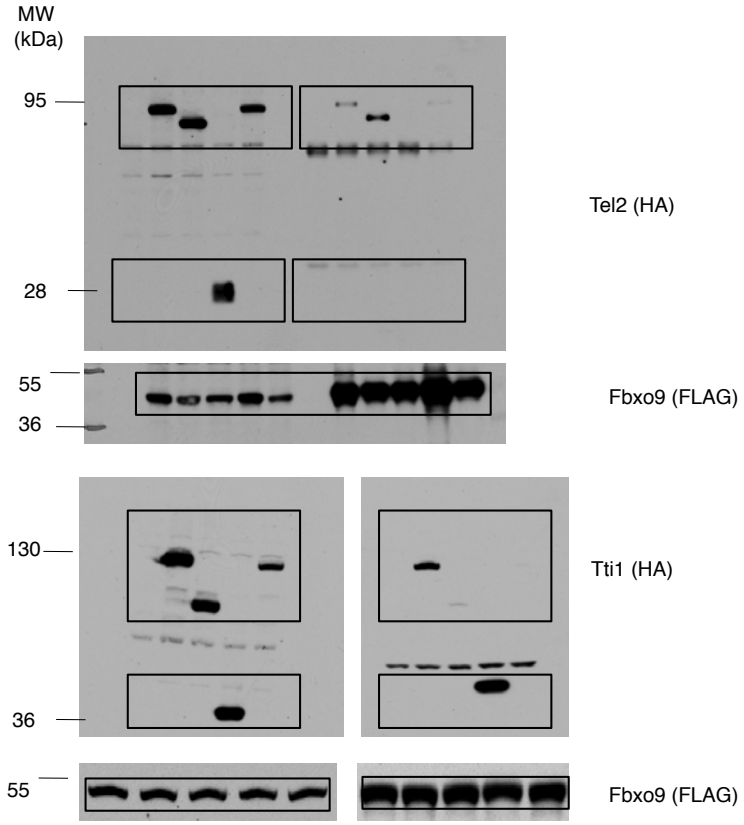

Figure 2b

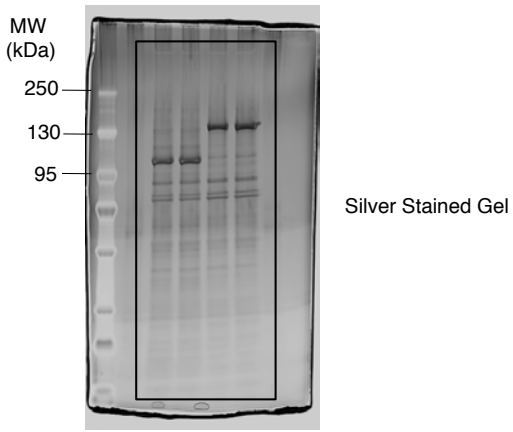

Figure S9 Full scans continued

Figure 2f

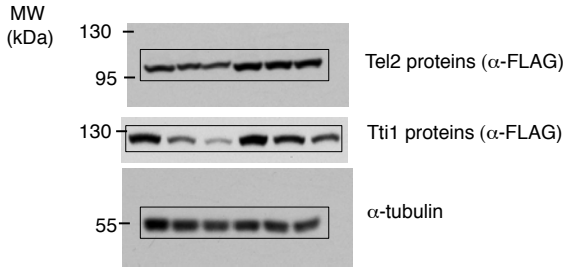

Figure 3a

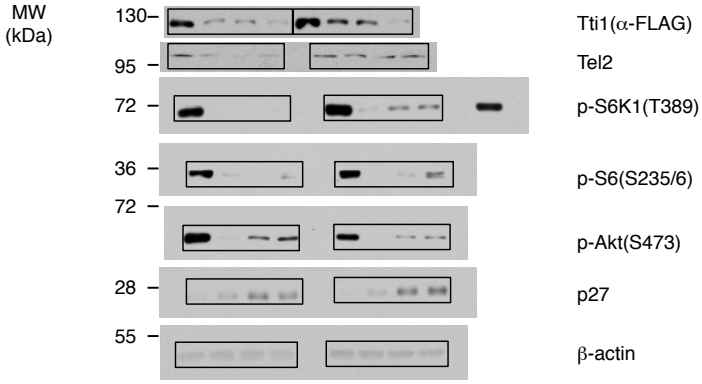

Figure 3d

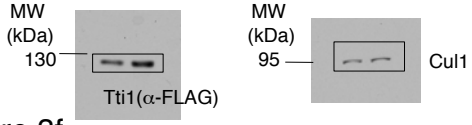

Figure 3f

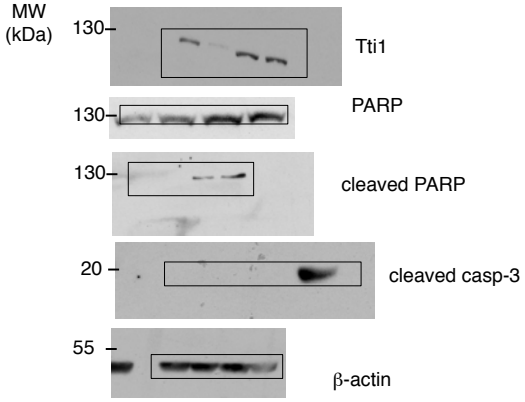

Figure S9 Full scans continued

Figure 3g

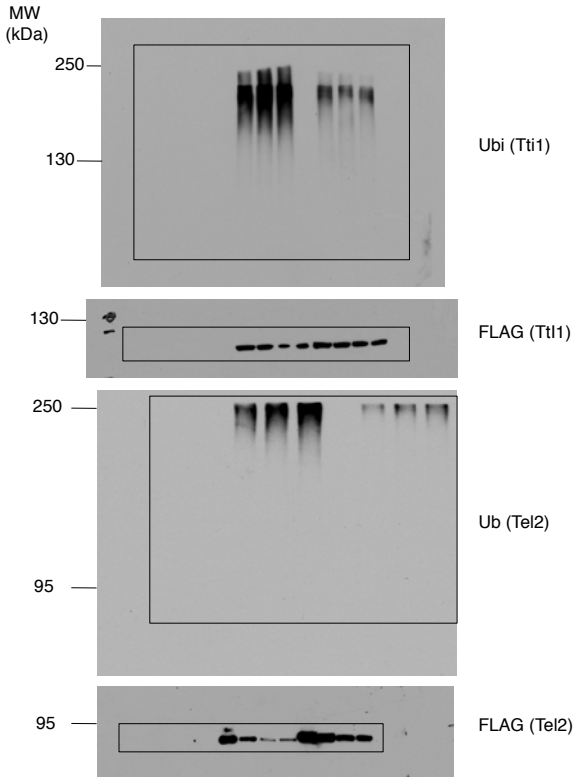

Figure 3h

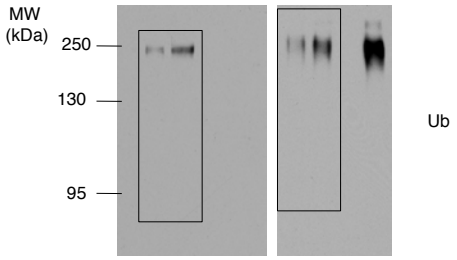

Figure S9 Full scans continued

Figure 4a

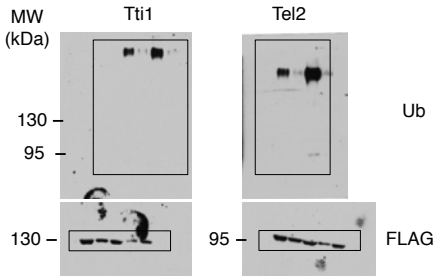

Figure 4d

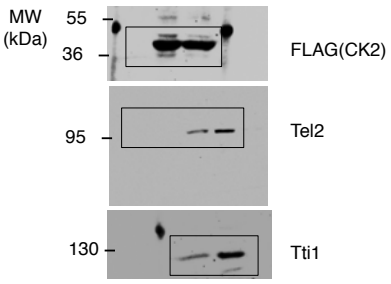

Figure 4e

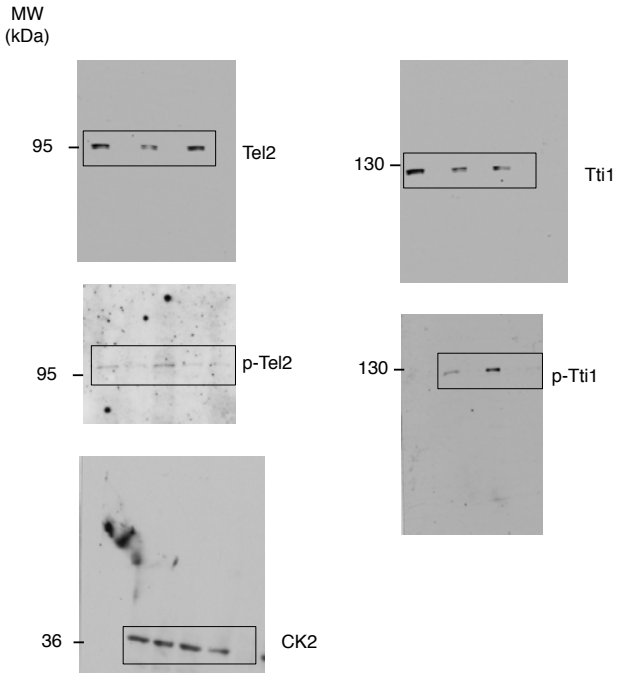

Figure S9 Full scans continued

Figure 4f

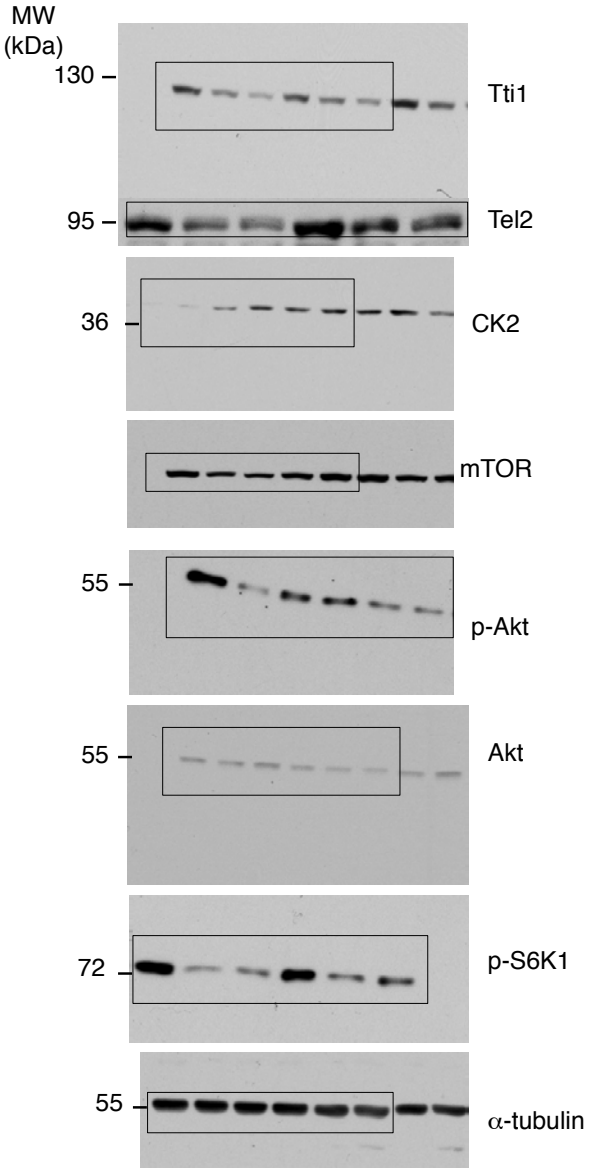

Figure 4g

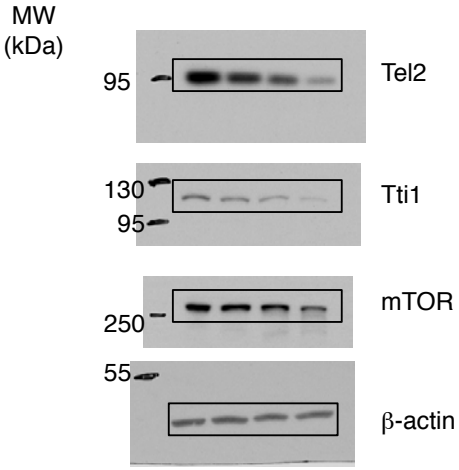

Figure 5a

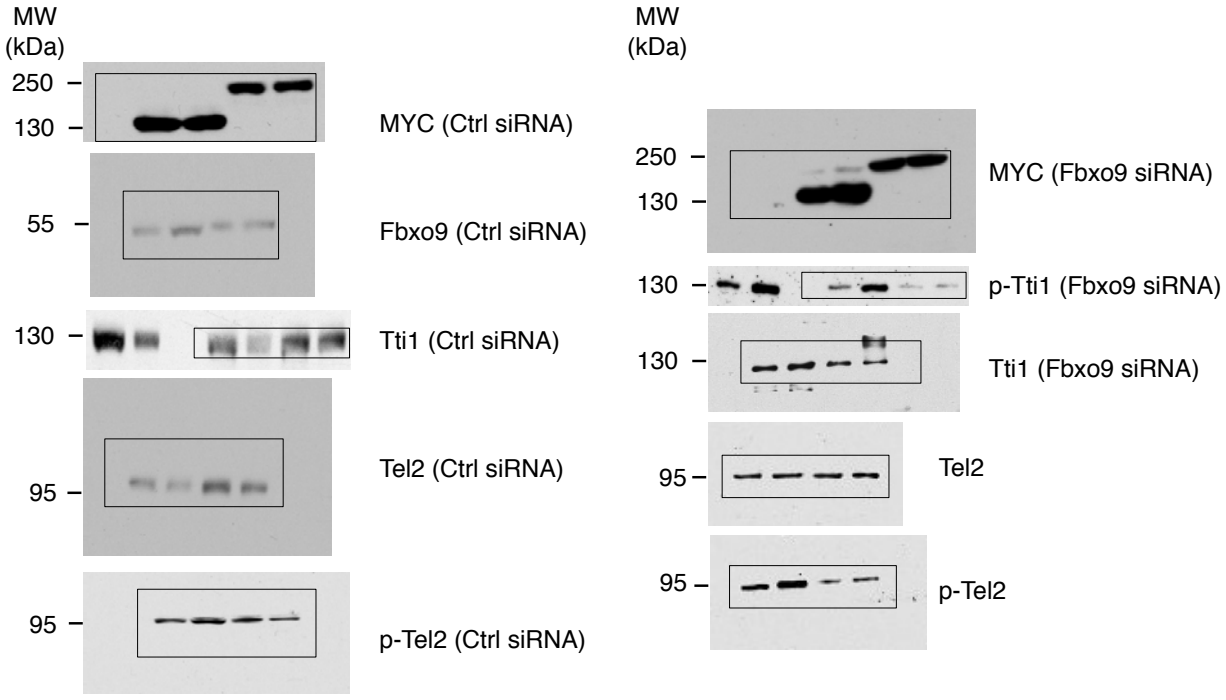

Figure 5c

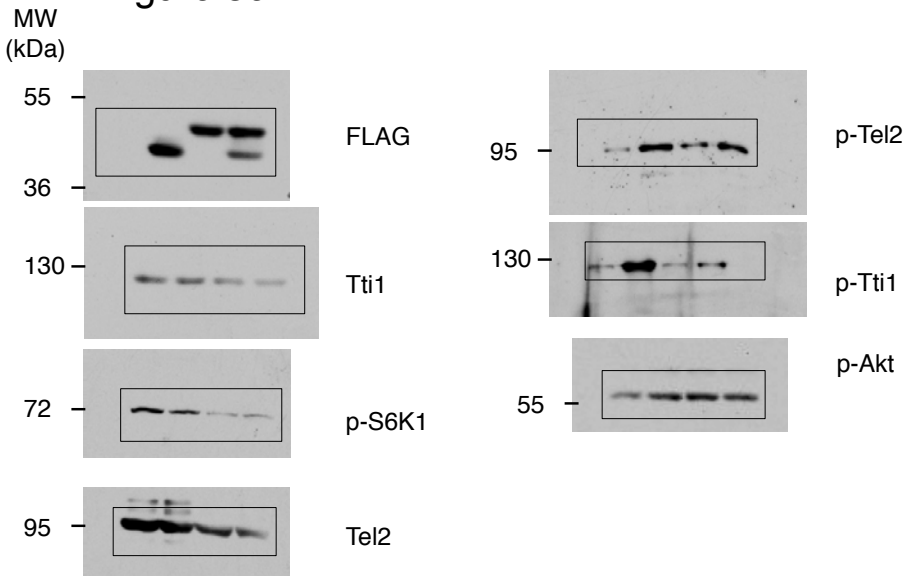

Figure 5d

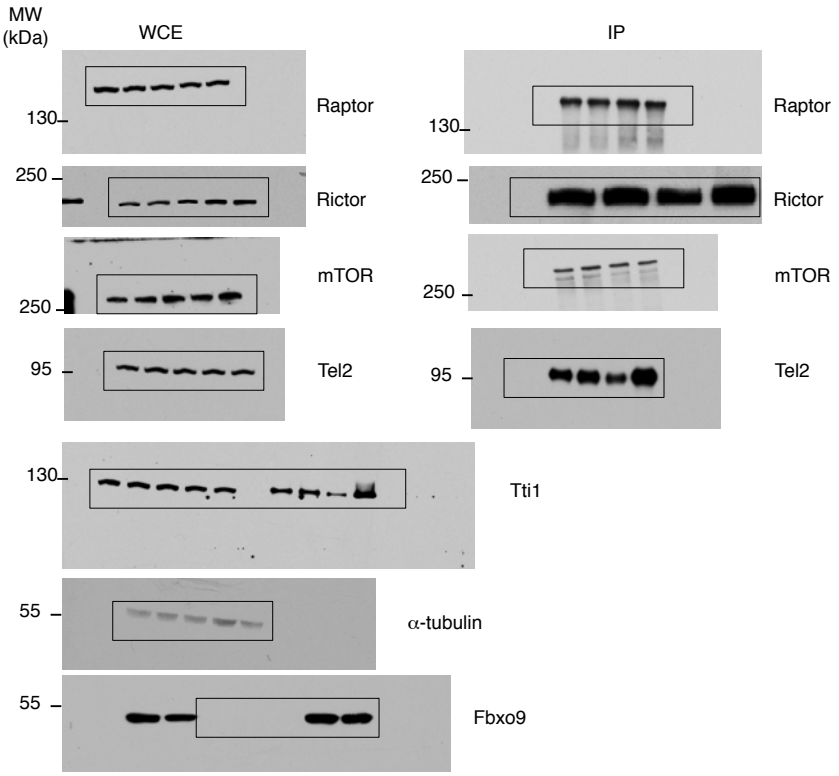

Figure 6a

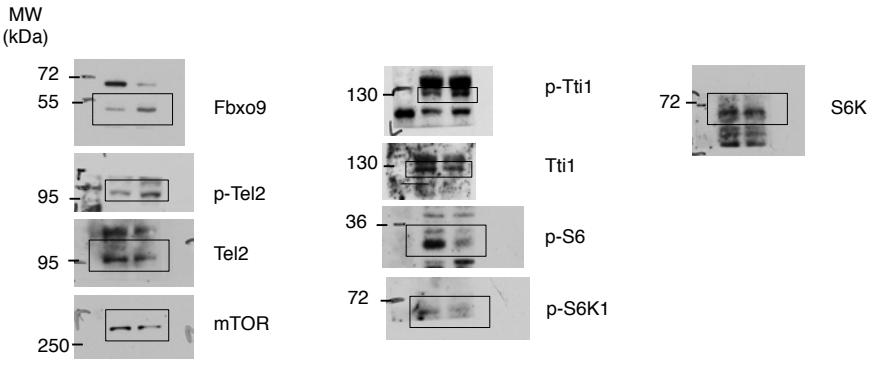

Figure S9 Full scans continued

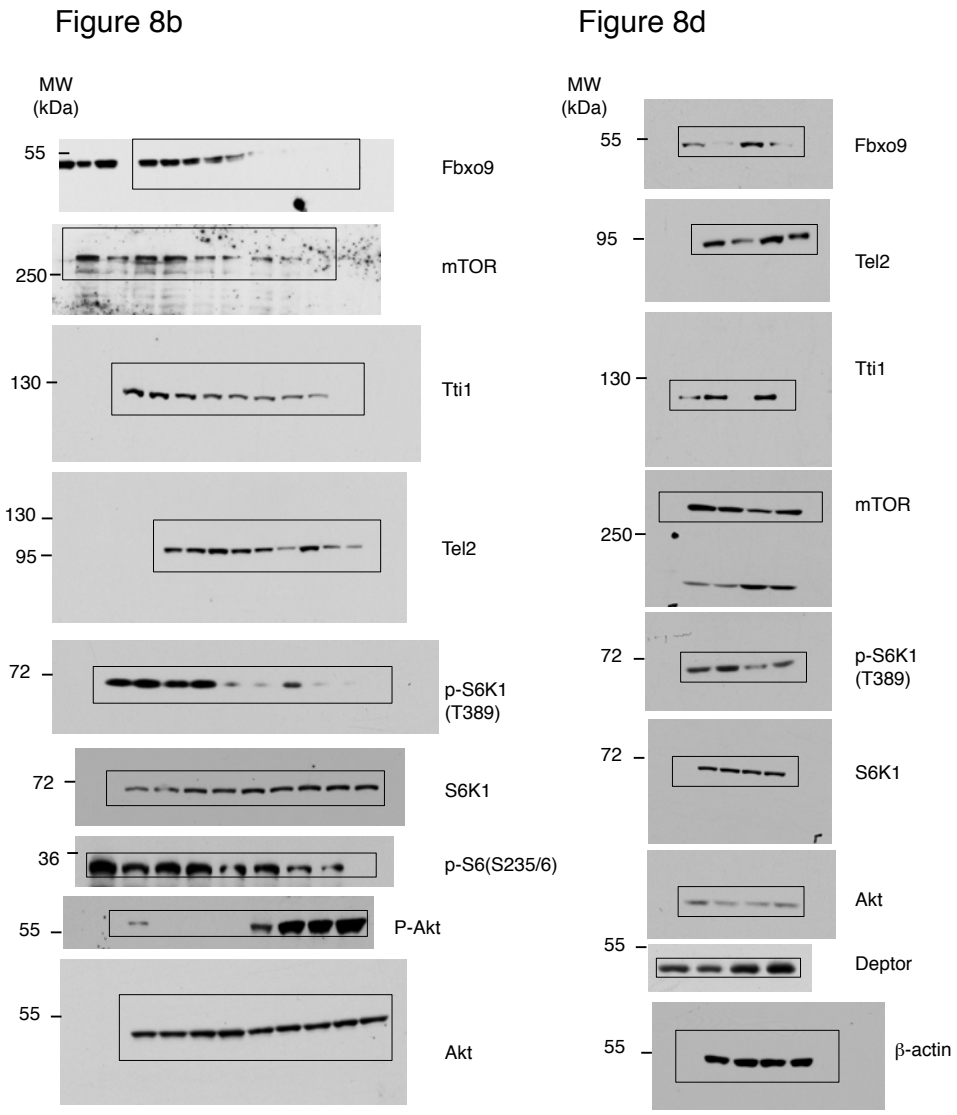

Figure S9 Full scans continued

Figure 8e

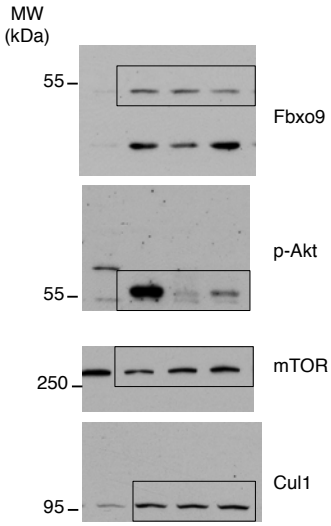

Figure 8g

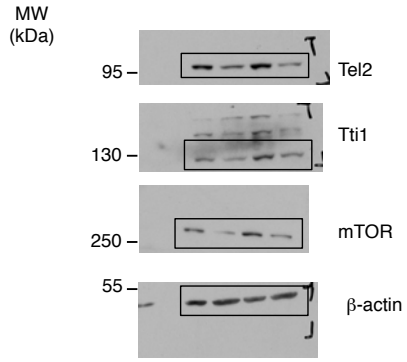

Figure 8f

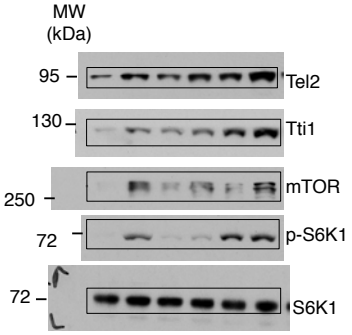

Figure S9 Full scans continued